CHAPTER 4

Smooth, All-Solid, Low-Hysteresis, Omniphobic Surfaces

This chapter is adapted from a first-author journal article published in *ACS Applied Materials and Interfaces*.[176] Kevin Golovin, Brian Tobelmann, and Omkar Gupte assisted with experiments.

4.1 Introduction

Hydrophobic or oleophobic surfaces prevent droplets of water or oil, respectively, from spreading across the surface, causing them to bead-up and, under certain conditions, roll or slide off. Omniphobic surfaces, on the other hand, possess the ability to repel a much broader range of liquids, regardless of their polarity or surface tension. Applications of omniphobic surfaces include "non-stick" coatings, bio- and mineral-fouling resistance, corrosion-prevention, chemical- and stain-resistance, prevention of protein and cell adhesion, and fouling-resistant printer nozzles.[8,101,177,178]

These surfaces may also be useful in applications where liquid mobility is required, such as in digital microfluidic devices and immersion photolithography, which uses a liquid droplet lens for high resolution patterning.[179,180] Patterning of omniphobic coatings enables the manufacture of non-wetting surfaces with wettable open channels for microfluidic devices,[181] as well as efficiency improvement in phase-change heat transfer and fog-harvesting applications,.[182,183] In the majority of these applications, the key requirement is that all liquids form mobile droplets on the surface that readily dewet without leaving any residue. The disparate strategies to achieve such repellent surfaces have yielded numerous surfaces with widely varying mechanical durability and effectiveness.[177]

As previously noted in Section 1.2, liquid droplets exhibit a range of contact angles on real surfaces ranging from θ_r to θ_a rather than the equilibrium Young's contact angle θ_E, due to heterogeneity in chemistry and roughness causing local variation in liquid-solid interactions. The difference between θ_a and θ_r is known as contact angle hysteresis ($\Delta\theta$). Ideally, an omniphobic surface should exhibit a low $\Delta\theta$ for essentially all contacting liquids, because minimizing $\Delta\theta$ reduces the tilting angle required to allow a droplet to slide on the surface, according to the Furmidge relation

(see Equation 1.2). Minimizing the $\Delta\theta$ with all liquids thereby enhances the liquid-repellency of an omniphobic surface.

Approaches to producing liquid-repellent surfaces include: fabricating rough surface textures that entrap air pockets beneath the liquid, infusing porous surfaces with immiscible liquid lubricants, and modifying smooth surfaces with reactive low-surface-energy molecules. These methods each have potential drawbacks, which limit their long-term stability, durability, and scalability for industrial applications, in addition to reducing applicable substrate materials.[177]

Textured superomniphobic surfaces with re-entrant texture, as discussed in Section 1.2, maintain a composite solid-air interface beneath liquids with a broad range of surface tensions. Droplets on these surfaces exhibit extremely high contact angles (approaching 180°), and minimal $\Delta\theta$, and therefore easily roll or even bounce off.[5,40,58] However, reliance on entrapped air to maintain the non-wetted Cassie-Baxter state makes such surfaces vulnerable to transitioning to a wetted Wenzel state under elevated pressure across the liquid-air interface (*e.g.*, due to droplet impact or immersion depth). This transition is more prone to occur with lower surface tension liquids, which exhibit lower contact angles.[58] The micro- and nano-scale features on these surfaces are also vulnerable to mechanical damage, which introduces defects that may cause irreversible wetting.[65,184] It is especially challenging to maintain the necessary re-entrant geometry for superomniphobicity after abrasion.[177,185] Past efforts to produce durable superomniphobic surfaces with low hysteresis have included monolithic fluorinated aerogels, which would not be practical for coating applications,[186] or layer-by-layer polymer-nanoparticle composite coatings which were only evaluated with light scratch tests.[187]

The pressure stability of textured superomniphobic surfaces may be increased by replacing the entrapped air with a relatively non-volatile, inert liquid lubricant, such as a perfluoropolyether or a silicone oil.[8,188] The surface chemistry of the porous material may be modified to enhance lubricant wetting, thereby enabling a broad range of immiscible liquids to essentially float on top of the surface. Liquid droplets exhibit significantly lower contact angles on these lubricated surfaces than on textured superomniphobic surfaces, but with comparably low hysteresis and improved pressure stability. The liquid lubricant also imparts limited self-healing capabilities, as it can flow into damaged regions on the surface.[8] However, the lubricant may be depleted over time due to evaporation or displacement by other liquids, especially under high shear flows.[189,190] In certain cases, interaction between the lubricating liquid and floating liquid droplets may accelerate lubricant depletion by allowing a small amount of lubricant to be removed with each liquid droplet that slides from the surface.[7,182] The porous substrate also remains vulnerable to mechanical damage, which reduces the stability of the lubricant film.

Alternatively, a smooth homogeneous surface with low surface energy may be produced by covalently grafting small molecules to smooth substrates. For example, a densely-packed liquid

repellent monolayer of trifluoromethyl (–CF_3) groups may be produced by the self-assembly of perfluoroalkyl compounds with a reactive terminal functional group, such as a thiol, carboxylic acid, or silane.[21,191,192] Low hysteresis can also be achieved with flexible grafted poly(dimethyl siloxane) chains, which yields a mobile liquid-like surface, but with much lower contact angles.[51] Near-perfect monolayers of these molecules may yield negligible hysteresis and essentially zero sliding angles with a broad range of liquids. However, achieving complete surface coverage with these molecules is challenging, and highly dependent on reaction conditions and substrate surface chemistry.[193] For example, silanes react well with hydroxyl-rich oxide surfaces such as silica, alumina, and titania, while thiols react well with noble metals such as gold.[194] Surface cleanliness and activation is critical to minimizing hysteresis, both of which can be dependent on the substrate roughness.

To address the aforementioned drawbacks of textured superomniphobic surfaces, lubricated surfaces, and self-assembled monolayers, we have developed an all-solid, omniphobic coating, that can be applied to a broad range of substrates via spin or dip coating, and is suitable for applications when liquid dewetting is desirable but high contact angles are not strictly required. These applications include self-cleaning and stain-resistant surfaces, immersion photolithography, droplet microfluidics, non-stick coatings, and enhancing heat transport during condensation. Previous approaches to smooth, all-solid, low-hysteresis coatings have included layer-by-layer deposition, polymer matrices incorporating lubricant domains, and sol-gel deposition of mixed silanes, which are relatively complex compared to a single spin- or dip-coat.[11–13] The coating in this work relies on the partial phase separation of a highly fluorinated molecule from a polymeric matrix to produce surfaces with low contact angle hysteresis ($< 15\ ^\circ$) for most liquids, including water, hexadecane, toluene, ethanol, and silicone oil, regardless of their polarity or surface tension. These liquids slide easily from coated surfaces without leaving any residue. The all-solid nature of the coating addresses the pressure stability and long-term performance concerns with textured and liquid-infused surfaces. Furthermore, the coatings are mechanically durable and can be applied to a broad range of underlying substrates.

4.2 Materials and Methods

4.2.1 Materials

4.2.1.1 Fluorinated Solvents

2,3-dihydrodecafluoropentane (Chemours Vertrel XF, also known as HFC-43-10mee, purchased from TMC Industries), dichloropentafluoropropane (Asahi Glass Asahiklin-225/HCFC-225ca/cb, purchased from Structure Probe), methoxynonafluorobutane (3M HFE-7100, purchased from Sigma Aldrich), and hexafluorobenzene (SynQuest Laboratories) were used to dissolve coating components.

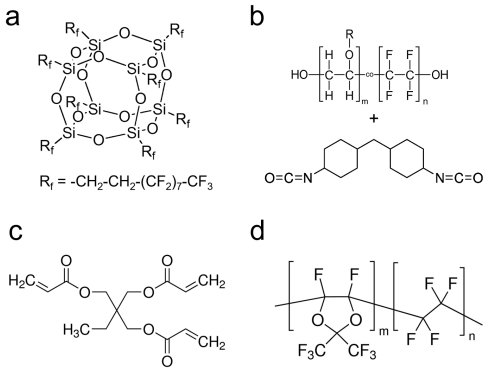

Figure 4.1: Structures of (*a*) F-POSS, (*b*) FPU polyol, and HMDI crosslinker, (*c*) TMPTA, (*d*) Teflon AF.

4.2.1.2 Contact Angle Probe Liquids

Deionized water (purified with a Pall Cascada RO filtration system), ethanol, n-hexadecane, n-heptane (Fisher Scientific), diidomethane (Acros Organics), and 5 cSt silicone oil (Sigma Aldrich) were used as contact angle probe liquids.

4.2.1.3 Hansen Solubility Solvents

In addition to the above, the following solvents were used for determining the Hansen solubility parameters of the coating components: chlorobenzene, ethylene glycol, n-Butyl acetate, o-Fluorotoluene, p-Chlorobenzotrifluoride, perfluorodecalin (Acros Organics), pentafluorobutane and tetrahydrofuran (THF) (Alfa Aesar), chloroform, dimethyl formamide (DMF), dimethyl sulfoxide (DMSO), hexane, methyl ethyl ketone (MEK), and toluene (Fisher Scientific), cyclohexane, dodecane, and diisopropylamine (Sigma Aldrich). Some of these were also confirmed to slide off the coatings, but the contact angles were not directly evaluated.

4.2.1.4 Polymer Components

Trimethylolpropane triacrylate (Polysciences) was mixed with 5 wt.% Irgacure 2022, a blend of UV radical photoinitiators (provided by BASF). Teflon AF 1600 was obtained from Chemours. Luxecolor 4FVBA fluorinated polyol resin (FPU, 55 % solids in n-butyl acetate) was purchased from Helicity Technologies. The isocyanate crosslinker, Wannate HMDI (4,4'-Diisocyanato-methylenedicyclohexane), was provided by Wanhua Chemical Group and added at 3.4 wt.%. Dibutyltin dilaurate (Sigma Aldrich), a catalyst, was added at 1 wt.% to accelerate cross-linking. The resulting partially fluorinated network polymer is referred to as FPU throughout the paper. See Figure 4.1 for the structures of the polymer components and that of F-POSS.

4.2.2 Coating Fabrication

Coating solutions were prepared at an overall concentration of 50 mg/mL in blends of fluorinated solvents (typically 1:1 HFC-43-10mee:HFB). The solutions were then vortexed until uniformly

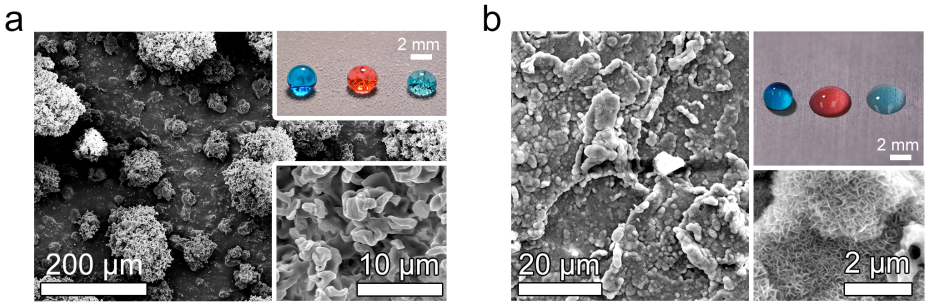

Figure 4.2: (*a*) SEM of the spray-coated textured superomniphobic surface, which is composed of large aggregates which are in turn composed individual dried droplets of FPU+50% F-POSS (*b*) SEM of the etched, boiled, fluorosilanized aluminum surface (prior to adding lubricant). It combines microscale texture from the hydrochloric acid etch process and nanoscale texture formed from boehmite crystals. Insets in (*a*) and (*b*) show SEMs at higher magnifications, as well as photographs of dyed ~15 μL droplets of water (blue), hexadecane (red), and ethanol (green) on these surfaces. The droplets on the textured superomniphobic surface are all in the Cassie-Baxter state, with entrapped air supporting them.

clear, then spin cast (using a Specialty Coating Systems G3P-8 spin coater. Recipe: ramp to 5,000 rpm in 1.5 seconds, hold 5 seconds, ramp down to 500 rpm and hold for 20 seconds, then stop) onto silicon wafer substrates (University Wafer). Prior to testing, TMPTA + F-POSS films were cured under 254 nm UV for 1 h. FPU + F-POSS films were cured for 12 h at 80 °C. Multiple coats of FPU + F-POSS were produced by spin coating multiple times, drying at 80 °C for 30 min between each step. Teflon AF, F-POSS, and their blends did not require subsequent treatment. The textured superomniphobic surface was produced by spraying FPU + 50% F-POSS, 50 mg/mL in pure HFC-43-10mee with an airbrush (Paasche VLS) onto a microscope slide. The coating was held at room temperature for 12 h to allow the solvent to evaporate completely, then cured for 2 days at 80 °C. See SEMs in Figure 4.2a. The lubricated surface was produced as follows. First, an aluminum substrate (6061 T6 alloy, McMaster-Carr) was etched in 2.5 M hydrochloric acid (Fisher Scientific) for 20 min, agitated in a bath sonicator for 10 minutes to remove aluminum particles, and was then placed in boiling water for 20 min to convert the outer layer to boehmite (γ-AlO(OH)) nano-crystals. The textured substrate was then reacted with a vapor of (heptadecafluoro-1,1,2,2-tetrahydrodecyl)triethoxy silane (Gelest) in a vacuum oven at ~5 mTorr and 80 °C for 24 h. Krytox GPL-100 perfluoropolyether oil (acquired from Miller-Stephenson Chemical Company) was then drop cast onto these now superhydrophobic substrates to produce a lubricated surface. Excess oil was removed by holding the samples vertically overnight. See SEMs of this surface prior to lubrication in Figure 4.2b.

4.2.3 Wettability Measurements

Advancing and receding contact angle measurements were performed with the sessile drop method using a Ramé-Hart 200 F1 contact angle goniometer. A ~10 μL liquid droplet suspended from

a dispensing needle was brought into contact with the substrate, and its volume increased and decreased to obtain the advancing and receding contact angles. A circular drop fit in the DROPImage Advanced software was used to obtain contact angle data. At least three points on the substrate were measured for each reported mean value. Standard error is ± 2°.

4.2.4 Construction of Hansen Solubility Spheres

This process was previously described in Section 3.3.1. Good solvents for F-POSS and Teflon AF were identified by attempting to dissolve them at concentration of 50 mg/mL in various solvents (Table 4.1). Miscibility parameters for the network polymers were obtained after they were cross-linked rather than with the small molecule components. This was done by performing swell tests. Small pieces of the cross-linked FPU and TMPTA with known masses were immersed in each test solvent for several days until a constant swollen mass was achieved. Hansen spheres were generated with the HSPiP software package and associated database of known Hansen solubility parameters for solvents. The miscibility parameter S^* for each polymer was then calculated as described in the main text.

4.2.5 Imaging and Metrology

Optical micrographs were obtained with a VWR VistaVision metallurgical microscope through crossed polarizers. Scanning electron micrographs were obtained with a Philips XL30 SEM after sputter coating the samples with gold to reduce charging effects. Coating thickness was measured by selectively scraping off the coating using a microtoming blade and using a Bruker Innova AFM with TESPA probes in tapping mode to measure the height of the step. Large area height maps (474 μm $\times$ 474 μm) were obtained with an Olympus LEXT OLS4000 3D laser measuring microscope and were used to measure root mean square average roughness (R_q) versus number of spin coated layers.

4.3 Results

4.3.1 Smooth Low-Hysteresis Films

Fluorodecyl polyhedral oligomeric silsesquioxane (F-POSS) was selected as the fluorinated additive in this work because of the high density of perfluorinated groups it possesses, in addition to its extremely low surface energy. F-POSS was produced using previously reported synthetic methods.[128] Unfortunately, F-POSS molecules typically form large crystals (tens of micrometers across) when deposited from solution, resulting in rough films with high contact angle hysteresis. For example, a solution of F-POSS was drop-cast onto silicon wafers from a solution of dihydrodecafluoropentane (HFC 43-10) and allowed to dry. The resulting surface showed high contact angle hysteresis with both water (θ_a/θ_r = 149°/110°) and hexadecane (θ_a/θ_r = 94°/49°). The production of smooth F-POSS films requires a volatile solvent with a high F-POSS solubility in order to delay precipitation and

Table 4.1: Solvent screening results used to construct Hansen solubility spheres.

Solvent	F-POSS	FPU (cross-linked)	Teflon AF	TMPTA (cross-linked)
Acetic Acid	×	✓	×	✓
Acetone	×	✓	×	✓
AK-225	✓	✓	✓	×
Chlorobenzene	×	✓	×	–
Chloroform	×	✓	×	✓
Cyclohexane	×	×	–	–
Diisopropylamine	×	×	×	–
DMF	×	×	×	✓
DMSO	×	×	×	✓
Dodecane	×	×	×	–
Ethanol	×	×	×	✓
Ethylene Glycol	×	×	×	–
HFB	✓	×	✓	×
Hexane	×	×	×	×
Hexanol	×	×	×	–
MEK	×	✓	×	×
n-Butyl Acetate	×	✓	–	–
o-Fluorotoluene	×	–	×	–
p-Chlorobenzo-trifluoride	×	–	×	–
Pentafluorobutane	×	–	×	–
THF	×	✓	×	×
Perfluorodecalin	×	×	✓	–
Toluene	×	✓	–	×
HFC-43-10mee	✓	×	✓	×
Water	×	×	×	×
δ_D (MPa$^{1/2}$)	14.26±0.10	16.04±0.2	13.76±0.10	20.65±0.35
δ_P (MPa$^{1/2}$)	0.03±0.80	9.45±0.45	0.09±0.95	10.79±1.20
δ_H (MPa$^{1/2}$)	0.03±1.15	3.55±0.45	0.06±1.25	12.97±1.25
R_o (MPa$^{1/2}$)	4.2	9.3	4.7	11.4
S^*	—	0.61	0.03	1.29

Table 4.2: Contact angles for F-POSS films spin coated from various fluorinated solvents, error is ±2°

Solvent	Water			Hexadecane			Ethanol		
	θ_a	θ_r	$\Delta\theta$	θ_a	θ_r	$\Delta\theta$	θ_a	θ_r	$\Delta\theta$
HFE-7100	124	112	12	80	72	8	73	61	12
HCFC-225ca/cb	130	114	16	80	68	12	74	60	14
HFC-43-10mee	128	112	16	80	64	16	73	57	16
10% HFB in HFC-43-10mee	129	119	10	81	70	11	75	62	13
15% HFB in HFC-43-10mee	129	119	10	81	71	10	76	63	13
20% HFB in HFC-43-10mee	129	120	9	81	72	9	75	64	11
30% HFB in HFC-43-10mee	126	121	5	81	75	6	75	66	9
40% HFB in HFC-43-10mee	125	121	4	80	77	3	75	70	5
50% HFB in HFC-43-10mee	124	121	3	80	77	3	75	71	4
60% HFB in HFC-43-10mee	124	120	4	79	76	3	74	69	5
70% HFB in HFC-43-10mee	124	121	3	80	78	2	75	70	5
80% HFB in HFC-43-10mee	125	121	4	80	77	3	74	69	5
90% HFB in HFC-43-10mee	128	120	8	81	72	9	75	63	12
HFB	128	117	11	81	70	11	75	63	12

minimize crystallization. Deposition was performed using a spin coating methodology (methods) to minimize the time available for F-POSS crystallization. The optimal solvent was determined to be an equal volume ratio mixture of HFC-43-10mee and hexafluorobenzene (HFB) (Table 4.2). The former is a highly volatile fluorinated solvent (boiling point 55 °C) with limited solubility for F-POSS (25 mg/mL), while the latter is less volatile (boiling point 80 °C), but is an excellent solvent for F-POSS (750 mg/mL). This 1:1 (v:v) solvent blend yielded films that were smoother and exhibited lower contact angle hysteresis than those spin cast from pure solutions of either solvent or alternative solvent mixtures.

Films of pure F-POSS spin cast at 5,000 rpm from 1:1 HFC-43-10mee:HFB exhibited very low contact angle hysteresis with liquids possessing a broad range of surface tensions and polarities, including water (θ_a/θ_r= 124°/120°), hexadecane (80°/77°), ethanol (75°/70°), and 5 cSt silicone oil (64°/59°) (Table 4.2). For all non-solvents of F-POSS, $\Delta\theta$ was ~5°, significantly lower than previously reported for pure F-POSS films, especially with low surface tension liquids.[59,128,195] The solid surface energy (calculated to be 10.1 ± 0.7 mJ/cm^2 using the Fowke's method) approached that of an atomically ordered trifluoromethyl monolayer (~9 mJ/cm^2), despite the evident nanoscale roughness of the film (Figure 4.3).[23]

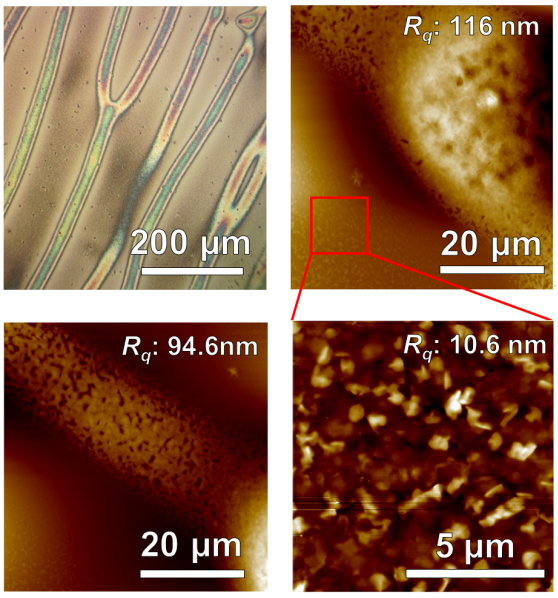

Figure 4.3: Optical micrograph and AFM scans of F-POSS spin coated in the ideal 1:1 blend of HFB:HFC-43-10mee.

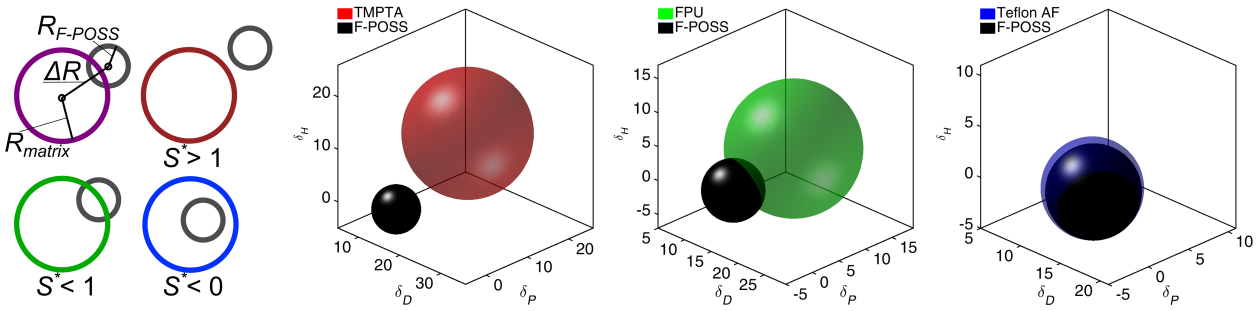

Figure 4.4: Hansen solubility spheres illustrating the miscibility between the F-POSS and TMPTA (immiscible, $S^* \approx 1.3$), FPU (partially miscible, $S^* \approx$), and Teflon AF (miscible, $S^* \approx 0.0$), polymer matrices.

4.3.2 Selection of a Durable Matrix Polymer

The low surface energy of F-POSS results in poor adhesion to substrates and limits its utility as a coating. Therefore, it is necessary to blend F-POSS with an inherently durable matrix. Selecting a suitable matrix polymer requires consideration of its miscibility with F-POSS and its solvents, as these factors determine the stability, durability, and liquid repellency of the resulting coatings. The previously reported S^* miscibility parameter (Equation 3.2) was again used to classify the three coating matrices tested in this work. As F-POSS is an extremely low surface energy material, any immiscibility with the matrix polymer will drive it to the surface of a blended film during deposition.

Three polymer matrices were selected with varying Hansen parameters, and therefore varying miscibility with F-POSS, as shown in the structural diagrams (Figure 4.1). All matrix materials were fully soluble in the HFC-43-10mee:HFB solvent blend at the concentrations tested, which is more critically necessary for consistent and uniform spin-coated films than for the rough spray-coated

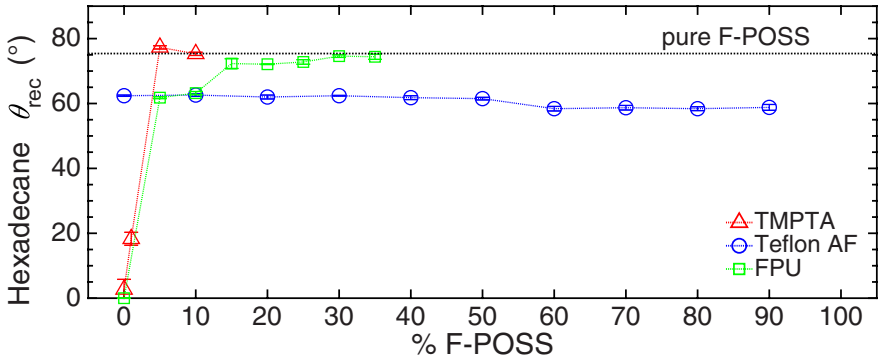

Figure 4.5: Receding contact angles with hexadecane for varying fractions of F-POSS in TMPTA, Teflon AF, and FPU. Error is ±2°. Note that the immiscible TMPTA based coatings reach the receding contact angle values for a pure F-POSS film at ~5 wt.% F-POSS, the partially miscible FPU based coatings reach those values at ~30 wt.% F-POSS, while the miscible Teflon AF based coatings never yields receding contact angle values obtained for F-POSS films.

surfaces produced in the previous work. Films of each polymer with varying fractions of F-POSS were spin coated and their liquid repellency and durability evaluated. As there is no broad consensus in the literature for method of testing durability of liquid-repellent surfaces,[185] we selected a commonly used standard methodology for testing the abrasion and scratch resistance of coatings. This automated abrasion test was performed with a Taber Model 5750 Linear Abraser using an CS-5 abrasive felt insert (~0.5 inch diameter), with approximately 250 g of applied load, equivalent to 20 kPa of pressure. This moderate load was selected such that the relative durability of the samples tested could be well-distinguished. The abrading head was reciprocated over the sample surface at 60 cycles/min, with a stroke length of one inch. The contact angles of water and hexadecane were periodically measured on the surfaces during abrasion testing. The receding contact angle with hexadecane was taken to be representative of the ability of a surface to repel low surface tension liquids. A significant reduction in the receding contact angle during abrasion indicated either the low surface energy material or the entire coating had been removed from the substrate. A receding contact angle approaching zero corresponds to the point where the liquid cannot slide from the surface without leaving residue, regardless of tilting angle, and therefore this was taken to be the failure point. Abrasion was halted when a significant portion of the underlying substrate was exposed or when hexadecane no longer receded from the surface, or both.

The first matrix evaluated was trimethylolpropane triacrylate (TMPTA), a nonfluorinated UV-curable network polymer, which has negligible miscibility with F-POSS ($S^* \approx 1.3$) (Figures 4.4, Figure 4.1). Spin coating a blend of TMPTA with just 5 wt.% F-POSS yielded a film with contact angles approaching that of the pure F-POSS film discussed above (water θ_a/θ_r = 124°/115°, hexadecane 81°/78°), (Figure 4.5). This suggested that the F-POSS molecules completely migrated to the upper surface of the polymer film (the polymer-air interface), which was undesirable, as a loosely adhered thin film of F-POSS on a surface could easily be abraded away or delaminated with solvents.

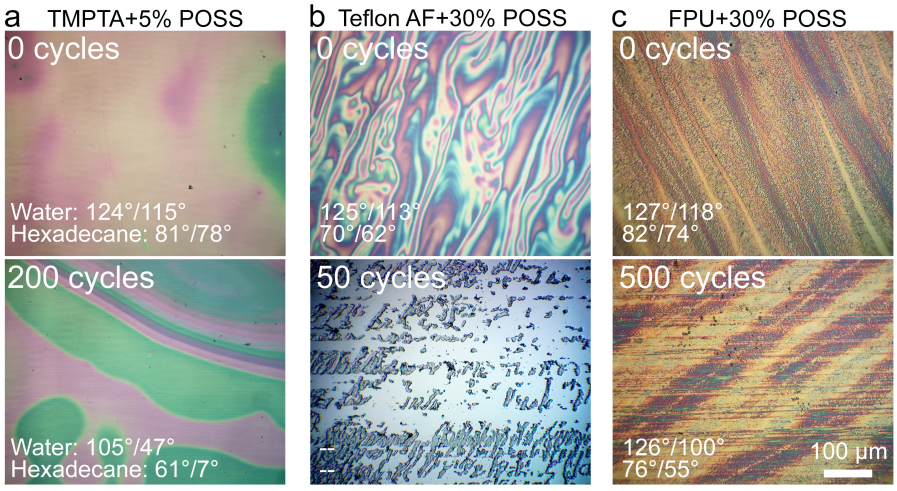

Figure 4.6: Comparison of abrasion between blends of F-POSS in TMPTA (*a*), Teflon AF (*b*), and FPU (*c*). Note that the TMPTA was not apparently physically damaged but the wettability changed significantly as the thin top F-POSS layer was removed, and the Teflon AF sample was physically damaged because it was not inherently durable. Meaningful contact angles could not be measured on Teflon AF after abrasion as the bulk of the coating was quickly removed.

This blended film lost liquid repellency after only 50 abrasion cycles (water θ_a/θ_r = 105°/47°, hexadecane 61°/7°), although the TMPTA matrix appeared undamaged (Figure 4.6).

By contrast, adding even up to 90 wt.% F-POSS in a highly fluorinated polymer which was completely miscible with F-POSS (Teflon AF, $S^* \approx 0$) did not yield contact angles equal to pure F-POSS (Figures 4.4 & 4.5). The maximum contact angles with hexadecane remained significantly lower than that of the fully fluorinated F-POSS monolayer (θ_a/θ_r = 70°/62° versus 80°/77°). This suggests that the F-POSS remained within the polymer matrix and did not completely cover the solid-air interface. Therefore, the $-CF_2$ groups present in Teflon AF raised the overall surface energy of the film (approaching 19 mJ/cm^2) versus a dense $-CF_3$ monolayer (< 10 mJ/cm^2).[196] Although pure Teflon AF still exhibited reasonably low contact angle hysteresis and high contact angles (water θ_a/θ_r = 125°/113°, hexadecane 69°/62°), it was not inherently durable, and films of this material and its F-POSS blends were completely destroyed after mild mechanical abrasion (< 50 Taber abrasion cycles; see Figure 4.6).

A partially fluorinated polyurethane (FPU; methods) yielded partial miscibility ($S^* \approx 0.6$). While phase separation did occur, receding contact angles approaching those of pure F-POSS films were not observed until > ~15 wt.% F-POSS (Figure 4.5), which indicated that a significant portion of the F-POSS molecules could be dispersed within the bulk of the film, reducing the surface energy throughout the composite film. A blend of FPU and 30 wt.% F-POSS exhibited contact angle values approaching that of pure F-POSS (water θ_a/θ_r = 127°/118°, hexadecane 82°/74°) (Figure 4.7a,b). This composite was also much more durable and better adhered to the underlying substrate, as demonstrated by the mechanical durability testing described below. As the surface possessed only

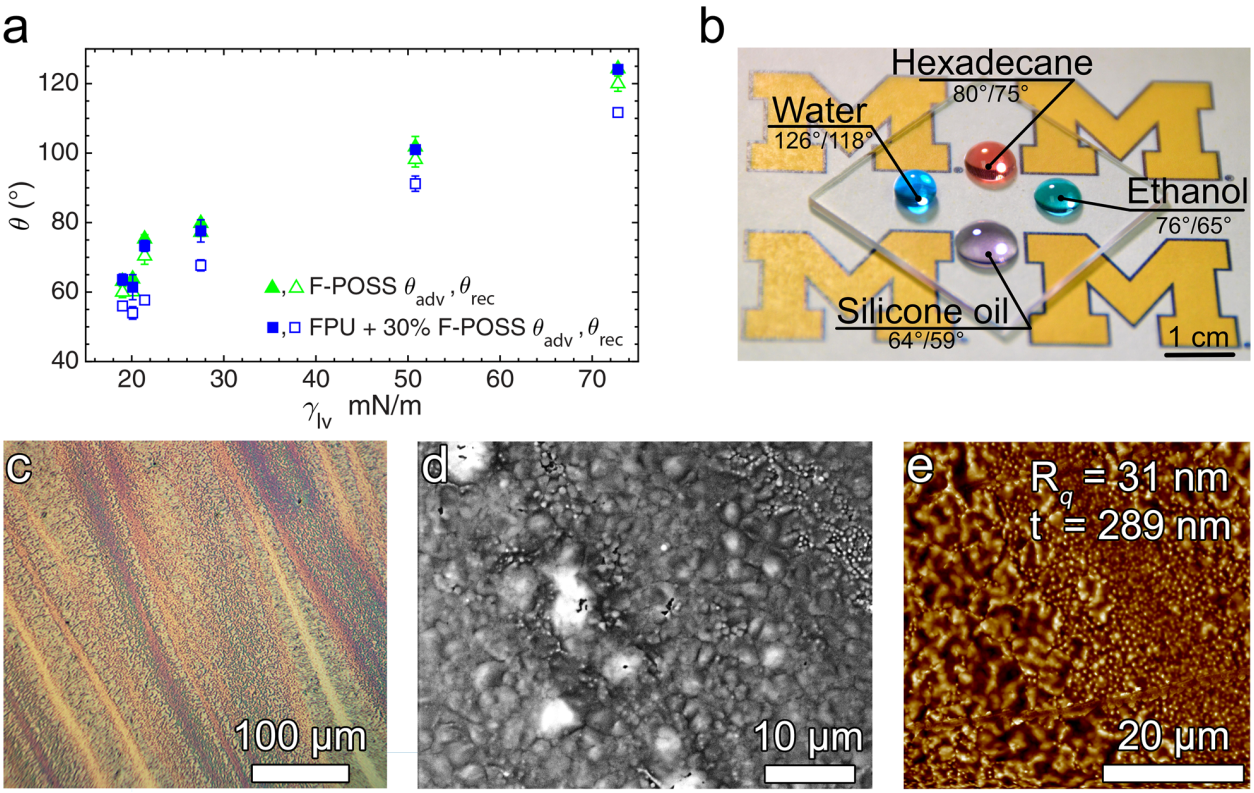

Figure 4.7: (*a*) Advancing and receding contact angles for liquids of varying surface tensions and polarities on spin coated F-POSS and FPU + 30% F-POSS films. Standard error is ± 2° (*b*) An image of various liquid droplets on a spin-cast film of FPU + 30% F-POSS film on top of a glass slide. The image highlights the transparency and non-wettability of the fabricated surfaces. All of these liquids will readily slide off the surface if it is tilted. (*c*) Optical micrograph, (*d*) SEM, and (*e*) AFM for a FPU + 30% F-POSS film.

nanoscale roughness and did not cause significant light scattering (Figures 4.7c-e), the FPU + F-POSS films were optically transparent (Figure 4.10a).

Virtually all high and low surface tension liquids slid readily on the surface, except for certain strong FPU solvents with low surface tension and high polarity (*e.g.*, tetrahydrofuran and acetone) as well as the most highly fluorinated solvents, which dissolve F-POSS. The coating was applied to a variety of smooth substrates: steel, aluminum, glass, polystyrene, poly(methyl methacrylate), in addition to silicon, and the contact angle hysteresis was consistently $< 11°$ for water and $< 9°$ for hexadecane (Table 4.3). High-speed spin coating was not critical for achieving low contact angle hysteresis, as dip coated films on silicon exhibited low contact angle hysteresis with both water (θ_a/θ_r = 129°/116°) and hexadecane (θ_a/θ_r = 81°/72°). This signifies that samples unsuitable for spin coating due to curvature or size could also be successfully coated (Table 4.4). For example, the coating was applied to the interior of small test tubes by simply filling them with the coating solution, then pouring it out. This treatment dramatically lowered the retention of dyed water and dodecane, as compared to the uncoated tubes (Figure 4.8).

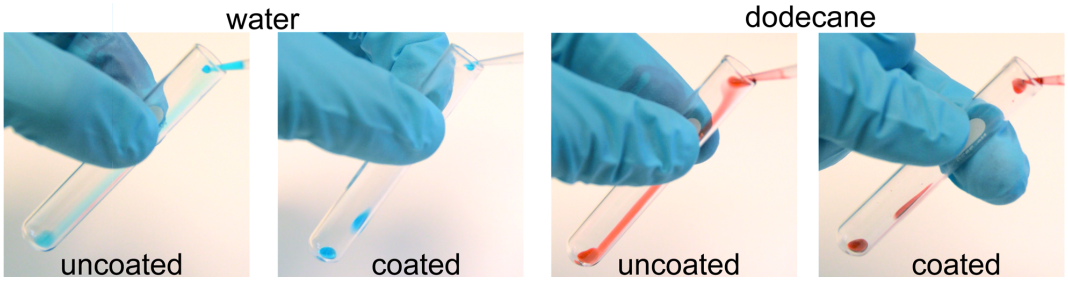

Figure 4.8: Images of water and dodecane being added to 5 mL glass test tubes which are uncoated or coated with FPU + 30% F-POSS. Note that the droplets do not wet the inner surface of the coated tubes.

Table 4.3: Contact angles for FPU+30% F-POSS films spun at 5,000 rpm onto various substrates, 50 mg/mL 1:1 HFC-43-10mee:HFB, contact angle error is ±2°

Substrate	R_q (nm)		Water			Hexadecane			Ethanol		
	Uncoated	Coated	θ_a	θ_r	$\Delta\theta$	θ_a	θ_r	$\Delta\theta$	θ_a	θ_r	$\Delta\theta$
Steel (polished)	79±4	71±4	125	114	11	80	71	9	76	62	14
Aluminum (polished)	147±33	95±1	125	114	11	81	74	7	76	62	14
Glass slide	11±1	56±1	125	115	10	79	71	8	75	60	15
Poly(methyl methacrylate)	24±1	53±3	125	115	10	81	76	5	76	65	11
Polystyrene	16±2	72±8	124	115	9	82	77	5	76	65	11
Silicon	< 10	31±2	126	116	10	81	73	8	77	62	15

Table 4.4: Contact angles for FPU+30% F-POSS films deposited onto silicon by various methods, 50 mg/mL 1:1 HFC-43-10mee:HFB, contact angle error is ±2°

Method	R_q (nm)	Water			Hexadecane			Ethanol		
		θ_a	θ_r	$\Delta\theta$	θ_a	θ_r	$\Delta\theta$	θ_a	θ_r	$\Delta\theta$
Drop cast	2200±200	128	107	21	82	62	20	76	46	30
Dip coated	116±60	129	116	13	81	72	9	76	59	17
500 rpm spin	60±3	129	116	13	82	73	9	76	61	15
1,000 rpm spin	57±1	128	116	12	81	74	7	76	61	15
2500 rpm spin	45±1	128	116	12	82	74	8	76	61	15
5,000 rpm spin	31±2	126	116	10	81	73	8	77	62	15

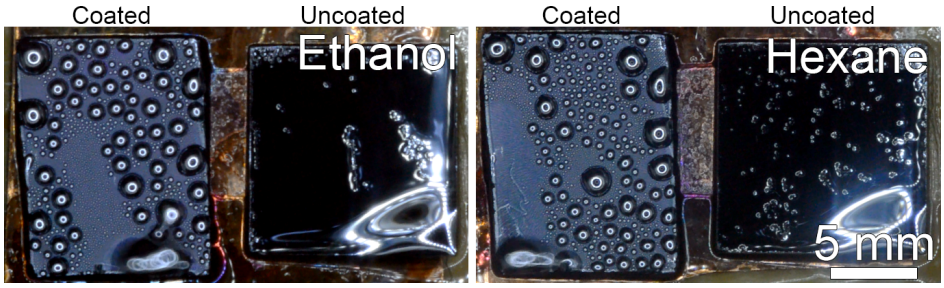

Figure 4.9: Condensation of ethanol and hexane onto cooled coated and uncoated silicon substrates under vacuum conditions. With both liquids, the uncoated substrate shows filmwise condensation. The blurred droplets in both images have just coalesced above the critical volume required for them to depart the substrate under gravity. Note the trail behind them filled with freshly nucleated small droplets.

4.3.3 Condensation of Low Surface Tension Liquids

Microscale droplets condensing from a vapor, particularly of a low surface tension liquid, may become immobile on both textured superomniphobic and lubricated surfaces. This is problematic for applications such as fog harvesting and condensation heat transfer.[182,197,198] To enhance heat transfer efficiency, it is desirable to maintain dropwise condensation behavior, as this increases the fraction of the cooled surface directly exposed to the hot vapor, as opposed to covered by the thermally insulating liquid. While the droplet nucleation rate is reduced with increasing contact angle, a low hysteresis surface is capable of regularly shedding droplets.

The condensation behavior of low-surface tension solvents on our smooth surfaces was evaluated in a lab-built vacuum chamber. The back wall of the chamber is actively cooled with ethylene glycol circulated through a copper heat transfer block, from a cooled bath (Penguin Chillers) pumped through a heated immersion circulator (Lauda-Brinkmann MS series) to precisely modulate the temperature. The sample was mounted to this wall with solvent-resistant double-sided tape (3M 9629PC). The solvent (ethanol, 99.5%, Sigma or n-hexane, 95%, Sigma) was placed into a glass beaker at the base of the chamber, in contact with three cartridge heaters which were controlled with a variable autotransformer, allowing the liquid temperature to be held at its boiling point. The chamber was sealed and pumped down to the minimum vacuum level, ~20 kPa and held at this level for ~15 min to evacuate non-condensable gases and water vapor. Then, the sample backside temperature was set to −10 ° C, and the cartridge heaters were turned on until the liquid began to boil. A stable equilibrium was reached with ethanol at $P \approx 25$ kPa and $T_{liq} \approx 45$ °C, and hexane at $P \approx 29$ kPa and $T_{liq} \approx 36$ °C. Dropwise condensation was observed for > 30 min in either case, with the continual removal of liquid and exposure of cooled surface (Figure 4.9).

4.3.4 Multiple Coats to Improve Durability and Reduce Hysteresis

The thickness, t, of the spin-coated FPU + 30% F-POSS could be increased by spin coating the solution multiple times on the same substrate (Figure 4.10b). Thicker samples should survive an

increased number of abrasion cycles before failure. This strategy of increasing coating thickness to improve abrasion resistance is not possible with lubricated surfaces or self-assembled monolayers. For textured superomniphobic surfaces, increasing the thickness to improve durability would only be effective if the initial re-entrant geometry could be preserved during abrasion, which is usually unlikely. Spin coating multiple times also yielded more uniform surfaces, leading to decreased contact angle hysteresis with water, hexadecane, and ethanol ($\Delta\theta$ decreases from 10° to 8°, from 8° to 6° and from 15° to 11°, respectively), concurrent with a decrease in the overall roughness of the coating (Figure 4.10b-e). This effect was more pronounced on substrates that were significantly rougher than silicon wafers, such as mill-finished steel and aluminum, as the coating material could fill in surface scratches. For example, coating rough steel substrates (R_q=1440 ± 80 nm) five times significantly decreased contact angle hysteresis of water, hexadecane, and ethanol when compared versus a single coat ($\Delta\theta$ decreases from 26° to 11°, from 21° to 7°, and from 47° to 21° respectively; see Table 4.5).

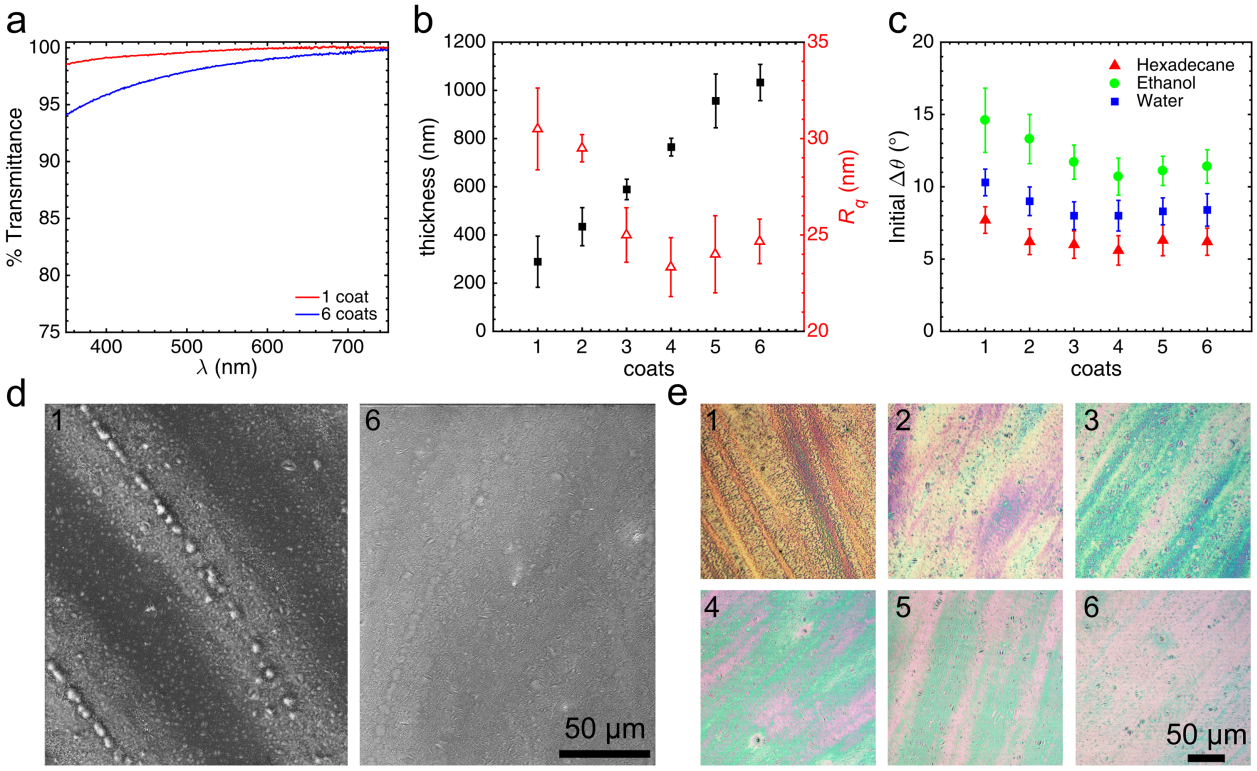

Figure 4.10: (*a*) High optical transparency is maintained even after multiple coats of FPU+30% F-POSS. (*b*) Multiple coats increase the film thickness, and increase the coatings mechanical robustness. A concurrent decrease in root-mean-squared roughness (R_q) was also observed using AFM measurements. (*c*) Reduced roughness yielded a decrease in the contact angle hysteresis with water, hexadecane, and ethanol (Table 4.5). (*d,e*) The reduced roughness and increased uniformity with multiple coats was also visible in SEMs and optical micrographs.

The abrasion resistance of our thickest FPU + 30 wt% F-POSS film (6 coats, t = 1030 ± 40 nm)

Table 4.5: Contact angles and roughness of FPU+30% F-POSS coated multiple times onto the same substrate, contact angle error is ±2°

Substrate R_q (nm)	Coats	Coated R_q (nm)	Water			Hexadecane			Ethanol		
			θ_a	θ_r	$\Delta\theta$	θ_a	θ_r	$\Delta\theta$	θ_a	θ_r	$\Delta\theta$
Silicon wafer <~10	1	31 ± 2	126	116	10	81	73	8	77	62	15
	2	30 ± 1	126	117	9	81	75	6	76	63	13
	3	25 ± 1	125	117	8	81	75	6	76	64	12
	4	23 ± 2	126	118	8	81	75	6	76	65	11
	5	24 ± 2	125	117	8	81	74	7	76	65	11
	6	25 ± 1	125	117	8	80	74	6	76	65	11
Unpolished aluminum 599 ± 141	1	475 ± 33	124	105	19	81	62	19	75	30	45
	2	433 ± 10	123	111	12	80	72	8	79	52	27
	3	405 ± 43	123	113	10	80	74	6	80	60	20
	4	364 ± 35	123	111	12	80	73	7	80	61	19
	5	367 ± 33	123	112	11	80	74	6	81	62	19
Unpolished steel 1440 ± 80	1	1371 ± 21	125	99	26	79	58	21	70	23	47
	2	1230 ± 46	125	105	20	79	65	14	74	36	38
	3	1220 ± 66	125	111	14	80	68	12	77	51	26
	4	1050 ± 120	126	115	11	79	70	9	76	52	24
	5	1100 ± 120	126	115	11	78	71	7	77	56	21

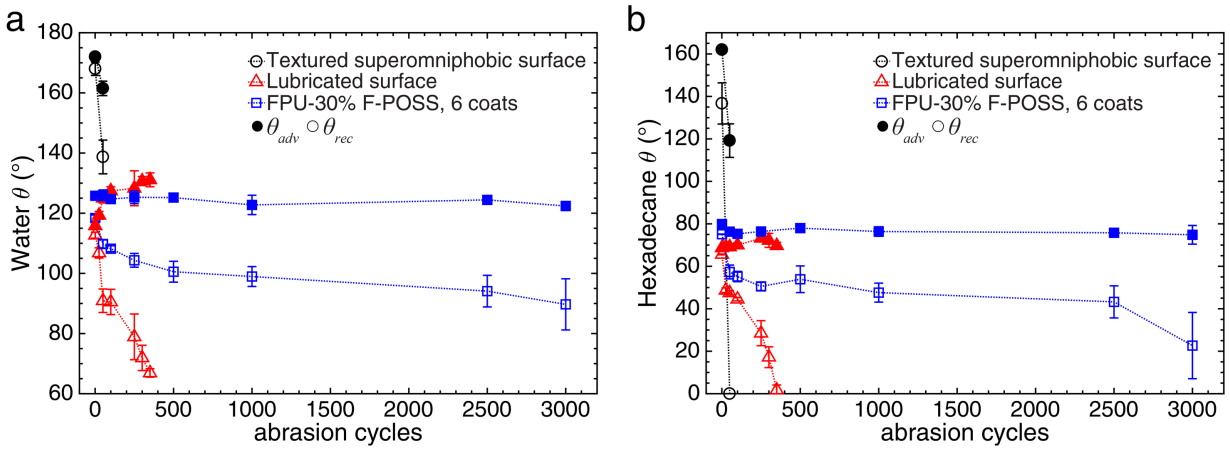

Figure 4.11: Advancing/receding contact angles of (*a*) water and (*b*) hexadecane versus linear abrasion cycles on a textured superomniphobic surface, a lubricated omniphobic surface, a spin-coated film of Teflon AF ($t \approx 200 \pm 50$ nm), and one coat ($t \approx 290 \pm 50$ nm) or six coats ($t \approx 1030 \pm 40$ nm) of the smooth omniphobic FPU+30% F-POSS coating.

was compared to that of was compared to the resistance of a thinner ($t = 290 \pm 50$ nm) single coat of FPU + 30 wt% F-POSS, a superomniphobic surface (FPU + 50 wt% F-POSS spray-coated with an airbrush), a lubricant-infused textured surface (perfluoropolyether drop-cast on an etched, fluorosilanized aluminum surface fabricated based on methods reported in literature),[139] and a spin-cast Teflon AF film (Figure 4.11; Figure 4.12; Figure 4.6). The Teflon AF, spray-coated, and lubricant-infused surfaces reached a zero receding contact angle with hexadecane relatively quickly during the abrasion testing (Figure 4.11), at 25, 50 and 350 cycles, respectively, but the FPU + 30 wt% F-POSS films maintained high contact angles significantly longer (after 2500 cycles on the sample coated six times, water $\theta_a/\theta_r = 123°/99°$, hexadecane 77°/50°). While low surface tension liquids completely adhered to the abraded textured and lubricated surfaces when inclined at 45°, they still slid from the FPU + 30 wt% POSS 6 coats sample when tilted after 350 abrasion cycles (Figure 4.12). Hexadecane remained mobile on the coating even after 1,000 abrasion cycles, as well as a number of other low surface tension liquids, including dodecane, ethylene glycol, and cyclohexanol, but ethanol and silicone oil did pin. As long as the coating remained free from macroscopic scratches, the contact angles with water and hexadecane remained relatively constant after an initial decrease. Coating failure due to scratching through to the substrate began to occur beyond 3,000 cycles in certain samples, but not until 8,000 cycles in others.

4.3.5 Other Durability Testing

A tape-peel adhesion test was performed, according to the ASTM D3359 standard, with the specified Elcometer 99 pressure sensitive tape.[199] Two sets of crossed scratches were made through the coating using a microtoming blade. The tape was adhered to the coating by applying pressure with an eraser, and then rapidly peeled off the surface as close to 180° as possible. The appearance of the coating

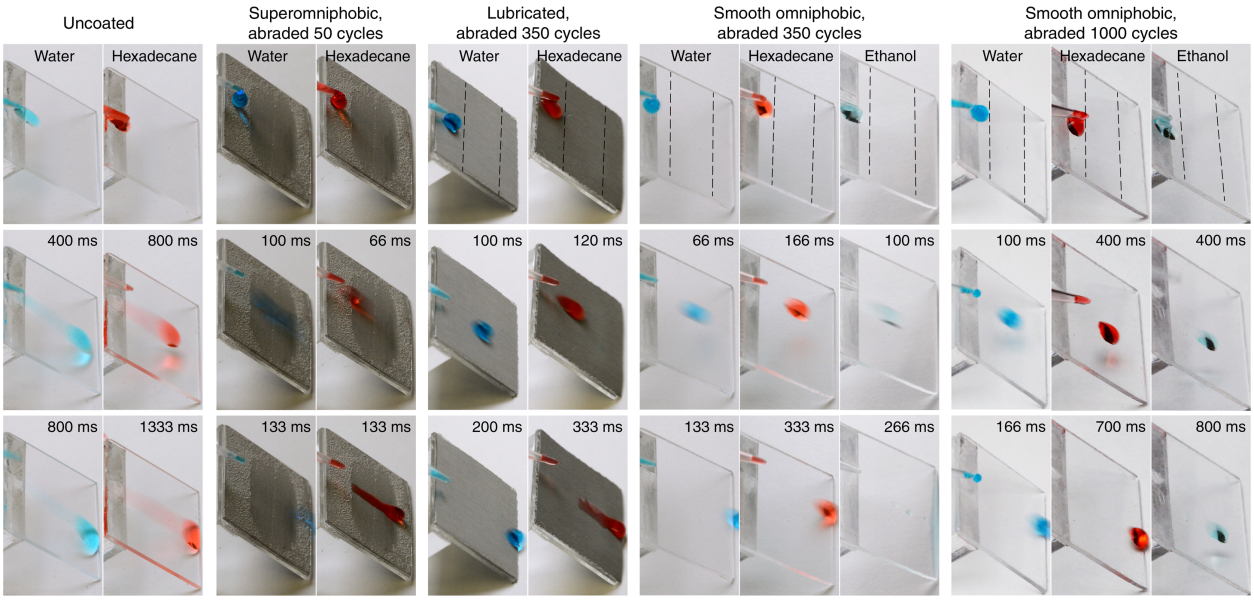

Figure 4.12: ~20 μL liquid droplets sliding on abraded samples inclined at 45°. The ~12.5 mm wide abraded track is located in the center of the 25×25 mm samples, perpendicular to the droplet sliding direction. Hexadecane readily wetted the superomniphobic and lubricated samples after 50 and 350 abrasion cycles, respectively, but slid on the thicker smooth omniphobic coating even after 1,000 cycles. However, ethanol, a polar low-γ_{LV} solvent, pinned irreversibly on the 1,000 cycle abraded sample.

was compared before and after testing. Contact angles were also measured after the test. This was performed on a sample coated six times to evaluate adhesion to a silicon substrate. No delamination was observed after peeling the tape from a scratched surface. The coating remained liquid repellent despite the apparent removal of some surface F-POSS molecules (initial: water θ_a/θ_r = 126°/118°, hexadecane 80°/75°, final: water 124°/107°, hexadecane 79°/59°).

A cyclic bending test on a 2.5 cm × 2.5 cm, ~120 μm thick polyester film coated six times with FPU + 30 wt% F-POSS, as described above. One end of the film, coating side upwards, was mounted to the linear abraser head, and the other was fixed in place. Each forward stroke of the abraser caused the center of the sample to buckle upwards, with a minimum bend radius of ~2.3 mm, as determined by comparing it to a glass rod of known dimensions. This radius was approximately the minimum radius prior to plastic deformation of the substrate material. Two thousand linear cycles on the abraser corresponded to one thousand bending events, after which there was no visible delamination or cracking of the coating. The contact angles in the bent area were virtually unchanged (initial: water θ_a/θ_r = 124°/113°, hexadecane 80°/73°, final: water 123°/111°, hexadecane 79°/71°).

4.4 Conclusions

We have demonstrated a facile, spin-coating methodology to produce highly liquid-repellent surfaces that allow liquids with a broad range of surface tensions and polarities to slide off without residue. We optimized the deposition of smooth coatings containing a highly fluorinated small molecule

(F-POSS), utilizing a blended fluorinated solvent to minimize crystallization, yielding surfaces with very low contact angle hysteresis with a broad range of liquids. An inherently durable fluorinated polyurethane in which the F-POSS is partially miscible was added as a matrix polymer in order to produce a mechanically durable omniphobic coating that adheres to a variety of substrates. The coating may also be applied to non-planar substrates via dip coating. The smooth, all-solid nature of the coating allows it to be inherently pressure stable, as well as more abrasion resistant than textured and lubricated omniphobic surfaces. This approach may facilitate novel applications where repelling all types of liquids from a transparent substrate is critical. These surfaces may be especially useful for displays, camera lenses, and microfluidic devices.

CHAPTER 5

Rapid and Robust Surface Treatment to Minimize Fouling by Liquids and Solids

Liquid or solid contaminants can foul surfaces and dramatically reduce their functionality. Numerous surface modifications have been demonstrated in the literature that reduce the adhesion of some solids or increase repellency to certain liquids, but are generally limited to specific contaminants. Here we demonstrate a rapid and facile surface modification technique that yields a thin film of liquid-like PDMS molecules tethered to a surface. This robust surface treatment resists the adsorption of a broad range of liquids with widely varying surface tensions and polarities, including water, oils, organic solvents, and even fluorinated solvents. Additionally, treated surfaces exhibit dramatically reduced adhesion to several types of solids, including ice, wax, calcined gypsum, and cyanoacrylate adhesive. This anti-fouling surface treatment may be broadly useful on surfaces found in architecture, transportation, biomedical, microfluidic, and photolithography applications. This chapter is adapted from an unpublished journal article co-authored with Kevin Golovin who developed the original idea and performed the initial experiments. Alex Kate Halvey and Abhishek Dhyani assisted with extending the experiments and finalizing the manuscript.

5.1 Introduction

Fouling, in its most general sense, involves a foreign contaminant adsorbing to a surface and compromising one or more of its desirable properties.[1] Fouling is a ubiquitous hindrance, including the bio-fouling of marine vessels,[200] the adhesion of dirt to apparel,[201] the accretion of ice on power lines,[202] and the adsorption of contaminants to water purification membranes.[4] Fouling can be subdivided into two categories: the unwanted adsorption of liquids or the unwanted adhesion of solids.

As discussed in Chapters 1 & 4, liquid-repellent materials may be classified by their ability to repel some combination of water, oils, and various high- and low-surface tension liquids (see Table 1.3). Highly textured surfaces maintain entrapped air pockets under the liquid, as in the case of superhydrophobic,[1,2,63,64,71] superamphiphobic,[5,57,58,113,203] or superomniphobic

surfaces.[47,60,204–206]

Lubricant-infused surfaces can also repel very low surface tension liquids with very low $\Delta\theta$, with improved pressure-stability and some inherent self-healing capability.[7,8,188] Both textured superomniphobic surfaces and lubricated surfaces may have limited longevity due to displacement of the entrapped air or lubricant, as discussed in Chapter 4. This may be accelerated by condensation of low surface tension liquids, droplet impact, high shear flows, or damage due to mechanical abrasion. As a more stable alternative, smooth and homogeneous solid omniphobic surfaces can also allow a broad range of liquids to be easily shed. They use a variety of fabrication methods, including polymers deposited from vapor or grafted in solution, spin-cast coatings with phase-separated low-surface-energy molecules or lubricant domains, or the deposition of various reactive small molecules such as alkyl or fluoroalkyl silanes.[11–13,51,52,59,128,198,207]

Similarly, various types of surfaces have been developed to resist the adhesion of solids, including lubricated systems,[8,208–213] soft rubbers,[214–218] omniphobic surfaces,[211,219] and hygroscopic polymers.[211,220] Some overlap exists.[8,59,208,219] The high interfacial area between an adherent solid and a wetted, textured surface may lead to extremely strong adhesion, so they are usually not ideal for resisting solid contamination.[221–223]

In general, there are no reported materials that simultaneously resist a broad range of liquid and solid contaminants. In principle, an ideally smooth and chemically homogeneous low surface energy material should exhibit a single equilibrium θ_E for each given liquid, with $\Delta\theta$ approaching 0°. However, in practice, most real surfaces exhibit $\Delta\theta > 10°$ with any liquid, and liquids with low γ_{LV} leave wetted films on most materials when removed. The surface may be made more ideal by reducing physical and chemical heterogeneity. Physical heterogeneity, or surface roughness, can usually be decreased through mechanical methods like polishing.[135] Chemical homogeneity, in contrast, is much more difficult to achieve.[59] Though self-assembled monolayers of low-surface-energy materials, such as fluoroalkyl thiols or silanes, may be made nearly homogeneous, they tend to be highly crystalline, causing any defects become locked into the structure and increase $\Delta\theta$. In contrast, tethering flexible, liquid-like molecules may produce fewer static defects. Such a mobile interface has been shown to drastically reduce $\Delta\theta$ with most liquids, and should also minimize the adhesion of solids.[51,52,224] In this work, we employ this strategy and present a facile method for fabricating films of flexible grafted polydimethylsiloxane and demonstrate their ability to drastically lower the adhesion of solids such as ice, wax, adhesives, and mud, and easily repel a broad range of liquids, including water, oils, organic solvents, and even ultra-low surface tension (γ_{LV}) fluorinated solvents.

5.2 Surface Treatment Methods

5.2.1 Grafted Bidentate PDMS

We have developed an extremely rapid, single-step, vapor-phase method to deposit an ultra-thin film of low-surface energy, liquid-like poly(dimethylsiloxane) on silicon wafers or glass. Exposing the silanol moieties on silicon wafers (University Wafer, P-type, test grade, 50 μm thickness, 1.5 nm native oxide layer, $\langle 100 \rangle$ orientation) to a room-temperature vapor of volatile, bi-functional, chlorine-terminated dimethylsiloxane for approximately ten minutes resulted in a stable, non-wettable, low-adhesion coating. Although various reaction times, temperatures, pressures, and chlorine terminated dimethyl siloxane precursors of various lengths (n = 2, 3, 4, 6, or 30–50, Gelest) were investigated, the optimized silanization procedure was a ten-minute exposure to the shortest precursor, 1,3-dichlorotetramethyldisiloxane, at room temperature and pressure (Figure 5.1). This was performed on silicon chips of ~1 cm^2 area by placing them in a closed 47 mm polystyrene petri dish along with 50 μL of the chlorine-terminated PDMS in a small polystyrene cuvette. After exposure, the pieces were rinsed in toluene, 2-propanol, and deionized water, then dried with compressed air prior to use. 1,3-dichlorotetramethyldisiloxane was optimal for producing low-$\Delta\theta$ surfaces in this manner due to its high vapor pressure (~1 kPa at 25 °C) and high reactivity. This treatment rendered the surface non-wettable to a broad range of liquids, including water, oils, and low surface tension solvents, even including some which strongly swell bulk PDMS, such as hexadecane or toluene (Figure 5.2, Table 5.1). While several prior works have demonstrated liquid-repellent surfaces based on grafted PDMS, none have been shown to repel such a broad range of liquids, or have been produced in such a rapid (< 10 minutes) and simple manner (room temperature vapor exposure without catalysts or surface pre-treatment).[51,52,225–227]

5.2.2 Wettability Measurement

We measured advancing and receding contact angles for probe liquids with a wide range of surface tensions and polarities on these surfaces, including many not previously investigated in the literature (Table 5.1).[51,52] Advancing and receding contact angle measurements were performed with the sessile drop method using a Ramé-Hart 200 F1 contact angle goniometer. A ~10 μL droplet suspended from a dispensing needle was brought into contact with the substrate, and its volume increased and decreased to obtain the advancing and receding contact angles. A circular drop fit in the DROPImage Advanced software was used to obtain contact angle data. At least three points on the substrate were measured for each reported mean value. The standard error was ± 2°. High purity probe liquids were used as received, and included: ethanol, hexadecane, dodecane, decane, octane, heptane, hexane, cyclohexane, and pentane (Fisher Scientific), diidomethane, formamide, and methoxyperfluorobutane (Sigma Aldrich), hexafluorobenzene (SynQuest), high and low molecular

weight perfluoropolyethers (Chemours Krytox GPL 100 and GPL 103, Solvay-Solexis Galden HT-55 and HT-110), dihydrodecafluoropentane (Chemours Vertrel XF), pentafluorobutane (Alfa Aesar), *o*-fluorotoluene, perfluorodecalin, and 4-chlorobenzotrifluoride (Acros Organics).

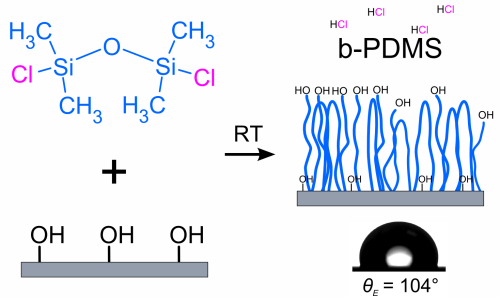

Figure 5.1: The proposed mechanism for the bidentate attachment of 1,3-dichlorotetramethyl-disiloxane. (*a*) a silicon wafer with surface silanol groups is exposed to the vapor of the silane at room temperature. The silane reacts with the silanol groups, as well as atmospheric water vapor, to yield grafted chains of poly(dimethyl siloxane) (PDMS). Hydrochloric acid is given off as a reaction product. The final surface is quite hydrophobic with the static water contact angle ~104°, but polar silanol groups remain on the surface and on chain ends.

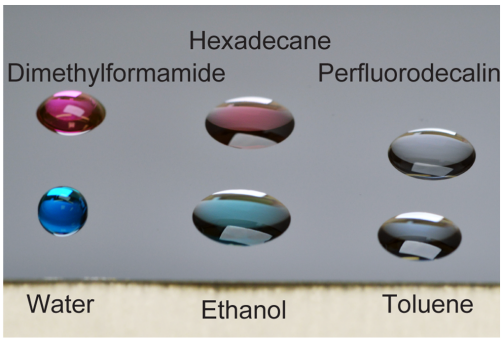

Figure 5.2: A photograph of liquids with broadly varying surface tensions and chemistries placed on a b-PDMS-treated silicon wafer.

5.2.3 Optimizing b-PDMS Film Thickness

Increasing the chemical homogeneity and decreasing the roughness of a surface reduces its contact angle hysteresis with all liquids. For these grafted bidentate PDMS films, denoted b-PDMS, this was achieved by controlling exposure time to the precursor, and thereby deposited thickness, which was determined with variable-angle spectroscopic ellipsometry (J. Woollam Co. M-2000). The measurements were performed in reflection mode using incidence angles of 55° through 75° in 5° increments. The data was fit using the CompleteEASE software. The optical constants of the silicon and native oxide were taken from values within the program, and the optical constants of the b-PDMS were determined using an experimental fit. The thickness of the b-PDMS film increased from < 1 nm after 30 seconds of exposure to > 6 nm after 1 hour of exposure. The minimum water

$\Delta\theta$ was achieved after 10 minutes, when the b-PDMS thickness reached ~4 nm (Figure 5.3). The lower θ_r and higher $\Delta\theta$ on samples exposed for less than 10 minutes most likely resulted from chemical inhomogeneity due to unreacted silanol groups on the silicon surface (Figure 5.1).

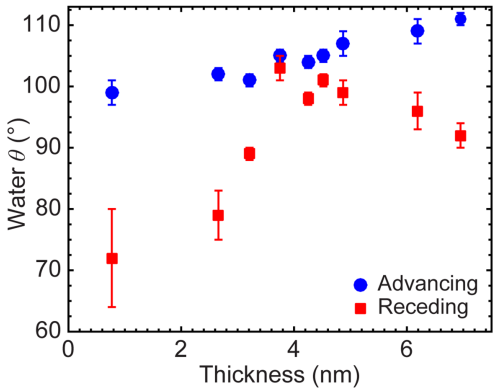

Figure 5.3: The advancing and receding water contact angles on the b-PDMS film as a function of thickness. Here the thickness was controlled by varying the exposure time to the silane (ranging from 30 seconds to 1 hour). Complete surface coverage was achieved at a thickness of approximately 4 nm.

Beyond the optimal 10 minute exposure, the θ_r again decreased along with significantly increased θ_a, raising $\Delta\theta$. This increase was likely due to an increased tendency towards self-polymerization of the b-PDMS rather than bidentate attachment to the substrate, resulting in higher roughness and the growth of longer molecules which have been previously shown to impede the motion of the three-phase contact line (Figure 5.1).[227]

To verify that the increase in $\Delta\theta$ was not caused solely by increasing film thickness, an optimal 4 nm thick b-PDMS sample was subjected to alternating cycles of 15 minute oxygen plasma treatments and 10 minute re-exposures to the precursor (Figure 5.4). Each oxygen plasma step hydrolyzed the surface methyl groups and rendered the surface completely wettable by water.[228,229] The resulting silanol groups were then reacted with the precursor to yield a b-PDMS surface with increased thickness, but the same $\Delta\theta$ as the original 4 nm thick surface. Repeating this procedure ten times yielded a 15 nm thick b-PDMS film that still exhibited $\Delta\theta \approx 2°$.

Low relative humidity ($< 30\%$) was found to be necessary to consistently produce the contact angles reported in Table 5.1. At higher humidity ($> 50\%$), typical water contact angles were 104°/99°. However, performing the same procedure under vacuum in a desiccator on days with high humidity resulted in contact angles equivalent to those of surfaces treated in air on low-humidity days.

5.2.4 Capping b-PDMS to Increase Contact Angles

Due to steric hindrance, bidentate silanes such as 1,3-dichlorotetramethyldisiloxane can only react with a limited portion of the silanol groups on a completely hydrolyzed silicon wafer, even for the

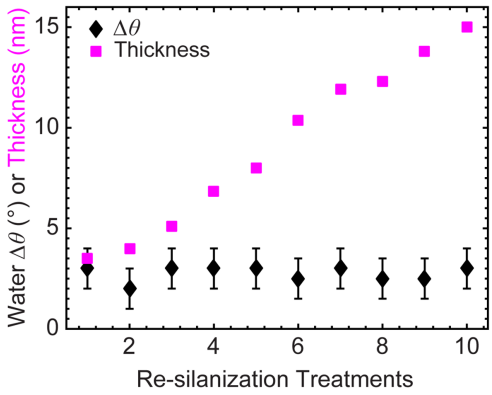

Figure 5.4: Exposing the optimal b-PDMS surface to O_2 plasma and subsequently re-silanizing the surface yielded a surface with identical $\Delta\theta$ to that prior to plasma treatment. However, the thickness was increased, and this could be repeated for at least ten subsequent exposures.

film with optimal surface coverage in Figure 5.3. Self-polymerization of the bidentate silane could also leave unreacted silanol groups within the b-PDMS film (Figure 5.1). Therefore, the surface energy may be further reduced by capping the residual silanol groups with a low molecular weight, monofunctional, hydrophobic silane such as trimethylchlorosilane. A b-PDMS treated wafer was placed in a closed container with 200 μL of trimethylchlorosilane (Sigma-Aldrich) for 1 hour. The sample was then washed with toluene and 2-propanol. We refer to this procedure as 'capping', and the capped, bidentate PDMS silanized surface as cb-PDMS. Whereas the b-PDMS surface exhibited $\theta_E \approx 104°$ with water, the cb-PDMS exhibited $\theta_E \approx 108°$ (Table 5.1), which approaches the intrinsic contact angle of a dense methylated surface, $\theta_E = 110°$ (Figure 5.5). This increase in θ_E with either unchanged or slightly improved $\Delta\theta$ was observed with most liquids (Table 5.1).[21]

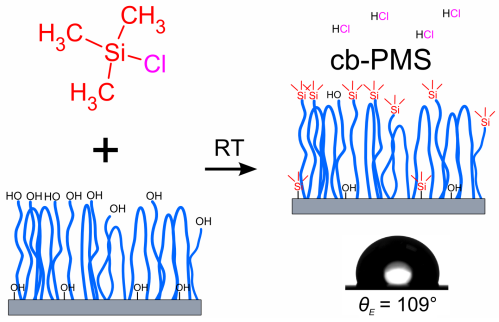

Figure 5.5: The wafer coated with b-PDMS is subsequently exposed to a vapor of trimethylchlorosilane, which converts most of the remaining silanol groups to fully methylated silicon atoms. The cb-PDMS exhibited static contact angles approaching the values reported for close-packed monolayers of trimethyl groups (~110°). Note that we show the likely case where complete reaction is not achieved, due to steric hindrance.

5.2.5 Modified Process for Glass Substrates

It is also desirable to produce low hysteresis surfaces on transparent substrates. Glass also has a silanol-rich surface which is highly reactive to the silanes used in this work. However, it was found that typical borosilicate glass required prior activation with oxygen plasma (Harrick Plasma PDC-001, RF power 30 watts, pressure ~200 mTorr for 30 min) and extended exposure times to the 1,3-dichlorotetramethyldisiloxane and trimethylchlorosilane (1 h and 3 h, respectively) to yield low $\Delta\theta$ approaching that on silicon. This modified process yielded dynamic water contact angles on 3" × 3" borosilicate glass substrates (McMaster-Carr) of 106°/101° for b-PDMS and 108°/102° for cb-PDMS.

5.2.6 Fluorinated Monolayer for Comparison

For comparison, we also vapor-deposited a monolayer of perfluorodecyldimethylchlorosilane (denoted F-17, Gelest) on silicon, since it is commonly used to produce non-wetting surfaces (Figure 5.6). The fabrication of this F-17 monolayer required a much more time- and energy-intensive process than the cb-PDMS grafted surface. First, the silicon wafers were pre-treated with O_2 plasma using a Harrick Plasma PDC-001 with an RF source power of 30 watts and a pressure of ~200 mTorr for 15 min. Note that we found that plasma cleaning did not improve b-PDMS silanization, and thus did not perform it for the PDMS surfaces on silicon. The plasma-cleaned wafer was then exposed for two 24 h periods to a vapor of perfluorodecyldimethylchlorosilane at 100 °C at < 5 mmHg in a vacuum oven. Prior to measuring contact angles or solid adhesion, treated substrates were thoroughly rinsed with isopropanol, Vertrel XF, and deionized water. Note that this mono-functional silane was selected to minimize self-polymerization and roughness, yielding films with optimal contact angles with low contact angle hysteresis approaching that of the b-PDMS. While the more commonly used perfluorodecyltrichlorosilane precursor will react faster, on the order of a few hours, it is prone to yielding rougher films, with typical water $\Delta\theta > 15°$.

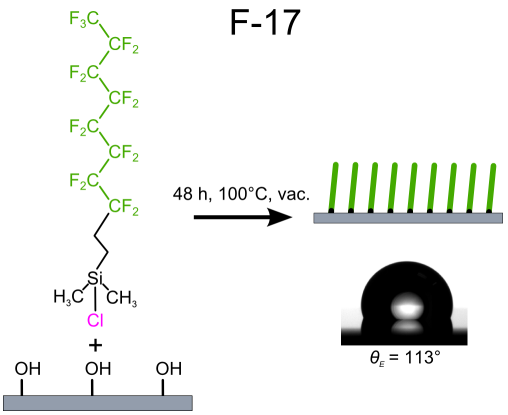

Figure 5.6: The deposition process for perfluorodecyldimethylchlorosilane, which yields a perfluorinated self-assembled monolayer.

5.3 Properties of Grafted PDMS Surfaces

5.3.1 Wettability

As expected, the F-17 monolayer exhibited higher contact angles with most liquids than the b-PDMS or cb-PDMS, as the surface energy of a perfluorinated monolayer (γ_{SV} ~9 mN/m) is lower than that of PDMS (γ_{SV} ~ 20 mN/m).[23,229] However, as long-chain perfluoroalkyl monolayers are highly crystalline, surface defects can act as pinning points even if γ_{SV} is relatively low.[191] For every probe liquid evaluated, $\Delta\theta$ for the F-17 monolayer was significantly higher than of either the b-PDMS or the cb-PDMS films. Fluorine-fluorine interactions are known to play a large role in the solvation of fluorinated species,[129,130] which was most likely the reason why several of the liquids did not recede from the F-17 monolayer. Moreover, we actually observed higher contact angles with the PDMS-based systems for perfluorodecalin and Krytox 100 (a short-chain perfluoropolyether),[8] which indicates very strong F-F interactions within the liquid and high interfacial tension between the liquid and the grafted PDMS. Typically, the surface tension of the highest surface tension liquid that fully wets a surface is a reasonable estimate of the surface energy of the solid, as first proposed by Zisman.[21] However, quite remarkably, we observed both a non-zero θ_r value and extremely low $\Delta\theta$ for liquids with lower surface tension than the solid surface energy of PDMS.

Table 5.1: θ_a/θ_r of various liquids on the fluorinated monolayer (F-17), bidentate PDMS film (b-PDMS), and capped bidentate PDMS film (cb-PDMS) on silicon.

Liquid	γ_{LV} (mN/m)	F-17	b-PDMS	cb-PDMS
Water	72.8	119°/109°	105°/103°	109°/107°
Dimethylformamide	37.1	80°/70°	65°/60°	68°/64°
Hexadecane	27.5	64°/58°	36°/35°	36°/35.5°
Toluene	28.4	65°/60°	26°/25°	32°/30°
Acetone	25.2	59°/53°	27°/26°	31°/30°
1-Propanol	23.7	56°/49°	24°/23°	33°/32°
Ethanol	22.1	55°/48°	26°/25°	32°/31.5°
Isopropanol	23.0	50°/44°	19°/11°	22°/19°
o-Fluorotoluene	28.0	68°/52°	28°/26.5°	27.5°/27°
p-Chlorobenzotrifluoride	24.0	61°/43°	25°/24°	25°/24°
Hexafluorobenzene	21.0	41°/35°	20°/18.5°	21°/21°
Perfluorodecalin	19.0	27°/23°	28°/27°	35°/34°
Krytox 100	16.0	23°/11°	32°/30°	32.5°/31.5°
Asahiklin 225	16.0	27°/17°	11°/10°	13°/12°
Pentafluorobutane	15.0	17°/0°	10°/10°	14.5°/14°
Vertrel XF	14.0	8°/0°	9°/9°	12°/12°
Methoxyperfluorobutane	13.0	12°/0°	10°/10°	14.5°/14°

5.3.2 Solid Adhesion

Various adherent solids were used to evaluate the solid-repellency of b-PDMS, including ice, cyanoacrylate adhesive, calcined gypsum, paraffin wax, and a PDMS elastomer. Ice adhesion is dependent on a material's ability to hydrogen bond with water molecules.[219] Metals, glass, ceramics, and hydrophilic polymers all display such a high affinity for the water molecules that the ice typically fails cohesively rather than detaching from the surface. The hydrophobicity of b-PDMS should minimize ice adhesion. The adhesion of other solid contaminants are less dependent on hydrogen bonding. We also evaluated the adhesion of cyanoacrylate superglue (covalent bonding), calcined gypsum (polar bonding), and paraffin wax (van der Waals interactions), and cross-linked PDMS elastomer to b-PDMS, cb-PDMS, and F-17 treated surfaces (Figures 5.7 & 5.8). Note that in all cases, the solid adherent started in a liquid state, resulting in complete solid/solid contact.

The adhesion force was measured using a lab-built shear force apparatus, as previously published (Figure 5.7).[215] For each test, a 1 cm × 1 cm × 1 cm poly(methyl methacrylate) cuvette, open at the top and bottom, was placed on the surface to be tested and filled with an adherent solid: ice, paraffin wax (PW, Sigma-Aldrich), cyanoacrylate adhesive (CA, 3M SF-100), calcined gypsum (CG, also known as plaster of Paris, Sheetrock Easy Sand 5), or polydimethylsiloxane elastomer (PDMS, Dow Corning Sylgard 184).

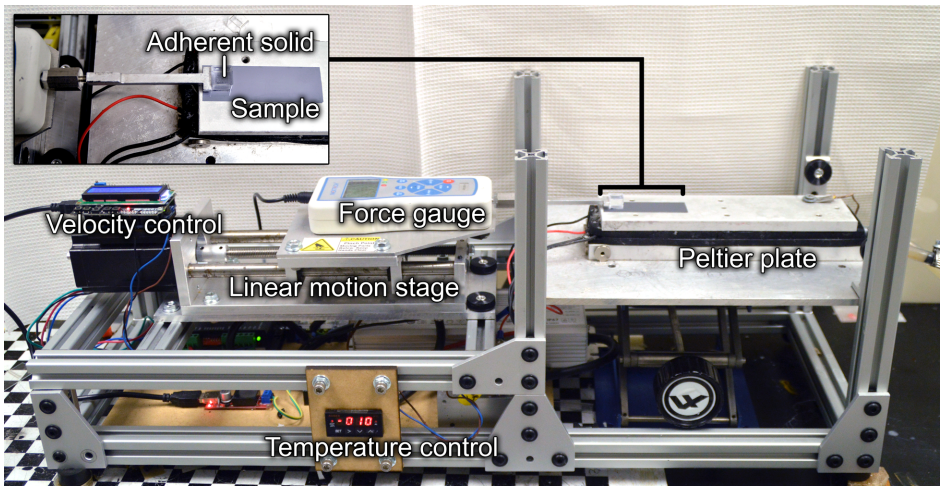

Figure 5.7: Schematic of the lab-built shear adhesion force measurement apparatus, which consists of a linear motion stage driving a force gauge against the side of a cuvette filled with a solid material adhered on a mounted sample substrate.

At least four measurements were performed for each material. In the case of ice, the surface was mounted to a peltier plate held at –10 °C and deionized water was poured into the cuvette and allowed to freeze to the surface. PW was melted at 150 °C on a hot plate, transferred to the cuvette on the substrate held at 50 °C, and then slowly cooled to room temperature. As CA only fully cures in thin layers, one face of a 1 cm^3 plastic cube was coated with the adhesive and placed

onto the sample surface and allowed to cure at room temperature. CG was prepared by mixing gypsum powder at 1 g/mL in deionized water for five minutes, pouring into the cuvette, and leaving overnight at room temperature, then heating at 50 °C for 3 h to fully harden. PDMS was prepared by mixing the base and crosslinker 10:1 by weight as recommended, and pouring into a cuvette on the surface on a 120 °C hot plate and curing for one hour. For each cuvette filled with each of the five materials, the tip of a force gauge mounted to a linear motion stage was brought into contact with one side of the cuvette ~1 mm above the base. A controlled shear rate (74μm/s) was applied to the cuvette until it detached from the substrate, and the peak force was recorded.

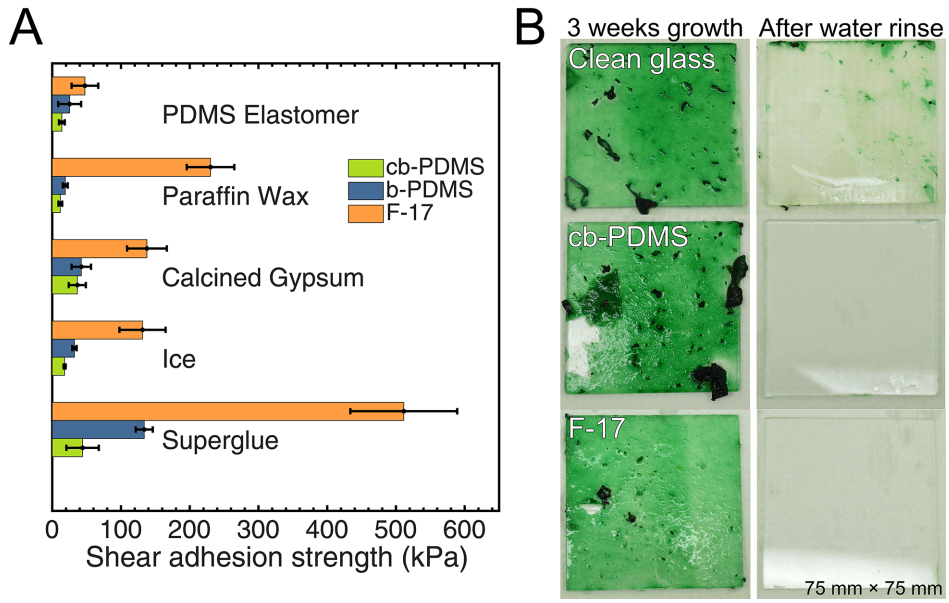

Figure 5.8: (*a*) The adhesion shear strength between five different solid materials on silicon wafers treated with b-PDMS, cb-PDMS, or F-17. All of the solids showed dramatically reduced adhesion to the liquid-like b-PDMS or cb-PDMS versus F-17. (*b*) Results of a three-week marine algae biofouling test. While algae strongly adhered to clean glass, gentle rinsing removed the bulk of the biofilm from F-17 and cb-PDMS surfaces. After wiping off the residual microalgae, however, the cb-PDMS retained lower contact angle hysteresis than the F-17 (water $\Delta\theta$ on cb-PDMS: 6° before, 11° after, versus on F-17: 12° before, 30° after).

Although perfluorinated surfaces exhibit lower surface energy than PDMS, the latter has been previously shown to better reduce solid adhesion, due to slip at the interface.[214,230,231] Similarly, we observed that the non-polar, liquid-like b-PDMS and cb-PDMS films reduced the solid adhesion significantly for all solids, compared to the F-17 monolayer, even for elastomeric PDMS adhesion.

5.3.3 Marine Biofouling

A fish tank was used to culture a mixture of marine diatom algae from four genera: *Amphora*, *Achnanthes*, *Entomoneis*, and *Navicula*, obtained from the United States Naval Academy. The water was adjusted to simulate marine conditions with Instant Ocean synthetic sea salt, with a final specific gravity of 1.015, and the nutrients and water level was replenished weekly. Three samples of 3" × 3"

borosilicate glass: a plasma-cleaned control sample, coated with cb-PDMS, and coated with F-17, were covered on one side with packing tape and placed horizontally, with the exposed side upwards, in the tank approximately two inches above the bottom. After they were left undisturbed for two weeks, the samples were carefully retrieved from the tank, and the tape was removed. Photographs and video were taken before, during, and after rinsing with deionized water from a squirt bottle to evaluate the ease of removal (Figure 5.8b). After immersion, all samples were coated with a soft filamentous biofilm. After rinsing, some areas of the plasma-cleaned glass substrate remained heavily coated, whereas the majority of the algal film on the cb-PDMS and F-17 samples was easily removed, as expected on low-$\Delta\theta$ surfaces.[232] Residual microalgae and bacteria remained on both samples. When this was completely wiped off, it was found that the cb-PDMS retained its non-wettability better than the F-17 (initial cb-PDMS water θ_a/θ_r = 108°/102°, final 105°/94°, versus initial F-17 water θ_a/θ_r = 115°/103°, final 101°/71°).

5.3.4 Liquid-like Monolayers

The glass transition temperature of PDMS is –123 °C, and at room temperature linear PDMS exists as a liquid which fully dissolves in relatively non-polar liquids like toluene and hexadecane.[233] Bulk, cross-linked PDMS swells in such liquids and displays $\theta_r = 0°$.[228] Why, then, did the b-PDMS film repel these solvating liquids (Table 5.1)? Two theories have been put forward. Cheng, *et al.* have suggested that the swelling of surface-bound molecules in miscible solvents, enhancing their liquid-like properties, is critical to achieving low hysteresis. They observed decreasing $\Delta\theta$ with increasing solvation of the PDMS chains in alkanes as opposed to polar liquids.[52] However, low-γ_{LV} liquids which are immiscible with PDMS, such as perfluorodecalin, still displayed $\Delta\theta \approx 1°$ (Table 5.1). Thus, swelling of the surface molecules is unlikely to be a necessary condition for low $\Delta\theta$. Alternatively, McCarthy *et al.* have suggested that the liquid-like nature of PDMS simply reduces solid/liquid interactions,[51] and therefore receding events, near the contact line. McCarthy has previously shown that even molecular topography can contribute to contact angle hysteresis.[225] Liquids can effortlessly dewet solid surfaces exhibiting a mobile interface, and if the surface is molecularly smooth, very low $\Delta\theta$ can be achieved. Additionally, this tethered liquid-like monolayer exhibits high interfacial slippage, naturally yielding the low solid adhesion strengths observed.

The viscous properties of the tethered molecules was studied by measuring the ice adhesion shear strength over a broad range of velocities. This was performed by pushing ice adhered on b-PDMS and cb-PDMS samples at linear velocities from 4μm/s to 2 mm/s (Figure 5.9). A strong dependence of the ice adhesion strength on the shear rate ($\dot{\gamma}$) was observed, indicating a large viscous component. The shear rate was defined as $\dot{\gamma} = v/h$, where v is the linear velocity and h is the measured b-PDMS thickness of 4 nm.[234] Linear PDMS is a shear thinning liquid at room temperature.[233] The shear stress, τ, for shear thinning liquids is known to follow a power-law dependence on shear rate over a

certain range, as $\tau = K\dot{\gamma}^n$. Here K is the consistency index, and n is the power law index (Newtonian fluids exhibit $n = 1$, and shear thinning fluids exhibit $0 \leq n \leq 1$).[235] Plotting τ vs. $\dot{\gamma}$ in logarithmic space (Figure 5.9b) allowed the determination of $K = 186$ Pa and $n = 0.58$ for b-PDMS, and $K = 187$ Pa and $n = 0.51$ for cb-PDMS. The good fits to a power law with n < 1 for both b-PDMS and cb-PDMS indicated behavior consistent with the known non-Newtonian shear-thinning behavior of liquid PDMS.

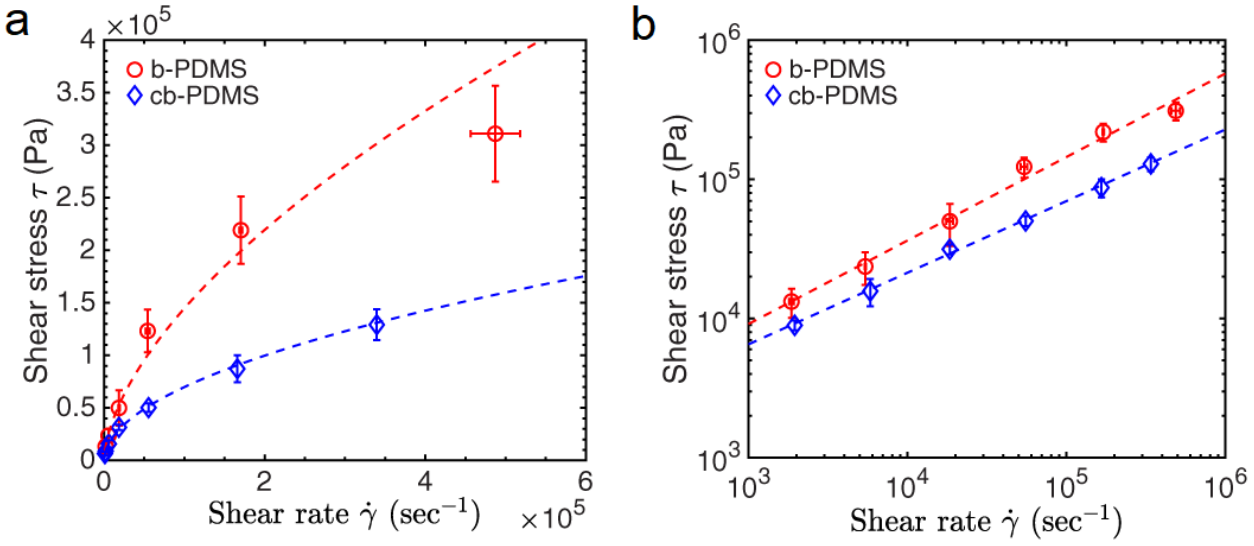

Figure 5.9: (*a*) The measured ice adhesion shear strength as a function of shear rate, for the b-PDMS and cb-PDMS surfaces. (*b*) When plotted in logarithmic space, a straight line was observed, indicating the power law regime of the viscous fluid.

K effectively represented the minimum possible ice adhesion strength observable on these two surfaces at infinitely low shear rates. It is recognized that there is typically an onset shear rate for the shear thinning behavior of PDMS.[236] However, the extremely thin film (4 nm) makes all practical velocities yield share rates well above the onset shear rate of ~1 s^{-1}. For example, even at a linear speed of 10 nm/s, $\dot{\gamma} = 2.5$ s^{-1}, therefore the onset shear rate could not be directly measured with our experimental setup.

5.4 Durability of Grafted PDMS

5.4.1 Solvent Exposure

As previously mentioned, lubricated surfaces employ a layer of liquid lubricant, typically perfluorinated, to repel other immiscible liquids with a wide range of surface tensions with $\Delta\theta \approx 2°$.[8] However, such systems cannot repel fluorinated liquids as the lubricants easily dissolve in these solvents, rendering the surface subsequently wettable even by higher surface tension liquids. To highlight the significant advantage of the cb-PDMS surfaces over a lubricated system, we placed

10 μL droplets of Krytox 100 (a representative fluorinated lubricant) on a cb-PDMS surface inclined by 0.5° (Figure 5.10). The cb-PDMS surfaces completely prevented wetting by this low γ_{LV} liquid (~16 mN/m), rather allowing it to slide around without leaving residue, maintaining a relatively high contact angle ($\theta_E \approx 32°$) and $\Delta\theta = 1°$.

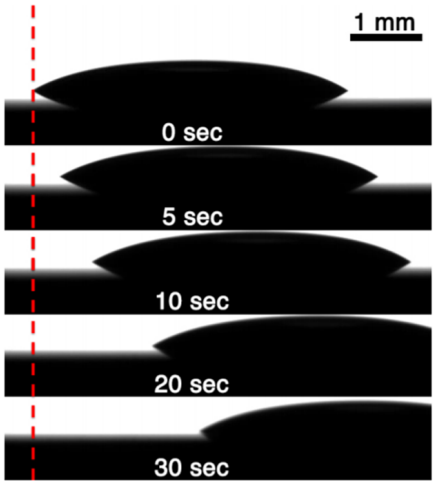

Figure 5.10: A droplet of Krytox 100 (a perfluoropolyether lubricant, γ_{LV} = 16 mN/m) was placed on the cb-PDMS surface at a tilt angle of 0.5°. The droplet easily slid from the surface, displaying negligible hysteresis, and did not leave a wetted trail.

We identified only a few liquids that can fully wet the b-PDMS and cb-PDMS films, including liquid linear PDMS, linear alkanes shorter than octane, small alkyl-amines, and ultra-low molecular weight perfluoropolyethers. These liquids exhibit a combination of very strong solubility for PDMS,[228] low molecular weight, and/or very low surface tension. However, unlike lubricated systems, where the repellency is lost when the lubricant is dissolved by a miscible solvent, the tethered PDMS films retained their ultra-low $\Delta\theta$ with other liquids after removal of the wetted solvent.

5.4.2 Other Damaging Exposures

To evaluate the robustness of the b-PDMS and cb-PDMS surface treatments against other harsh environmental conditions, we subjected the treated surfaces to a number of durability characterizations (Figure 5.11). Thermal testing was performed in air at 200 °C and 350 °C, and in boiling water or hexane. While $\Delta\theta$ did increase slightly, the films did not degrade completely even at these high temperatures. To ensure that the grafted surface was not easily damaged under mechanical abrasion, we subjected the b-PDMS and cb-PDMS films to 5,000 cycles of linear Taber abrasion using the CS-5 resilient felt abradant with a 250 g load (~20 kPa). The advancing and receding contact angles after abrasion for both water and hexadecane are shown in Figure 5.12. The contact angles deviated from their initial values by at most 1°. As the cb-PDMS thickness was only 4 nm, any surface degradation would result in a catastrophic contact angle decrease, especially for the receding angle

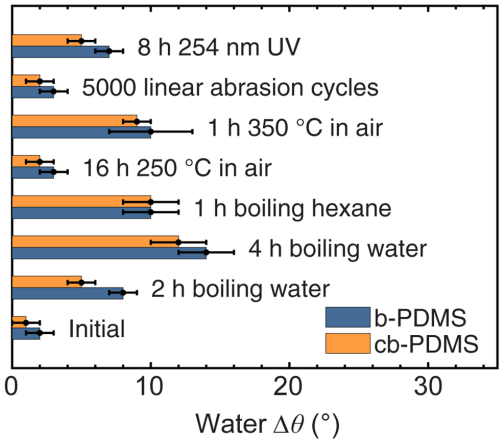

Figure 5.11: The water contact angle hysteresis of the b-PDMS and cb-PDMS after exposure to various harsh environments.

of hexadecane. This was not observed, indicating that this level of abrasion negligibly damaged the coating, with the water contact angles after 5,000 abrasion being θ_a/θ_r = 108°/106°. Compare this to the abrasion data for the previously described smooth omniphobic spin coated surface in Figure 4.11, which undergoes significant damage under these abrasion conditions.

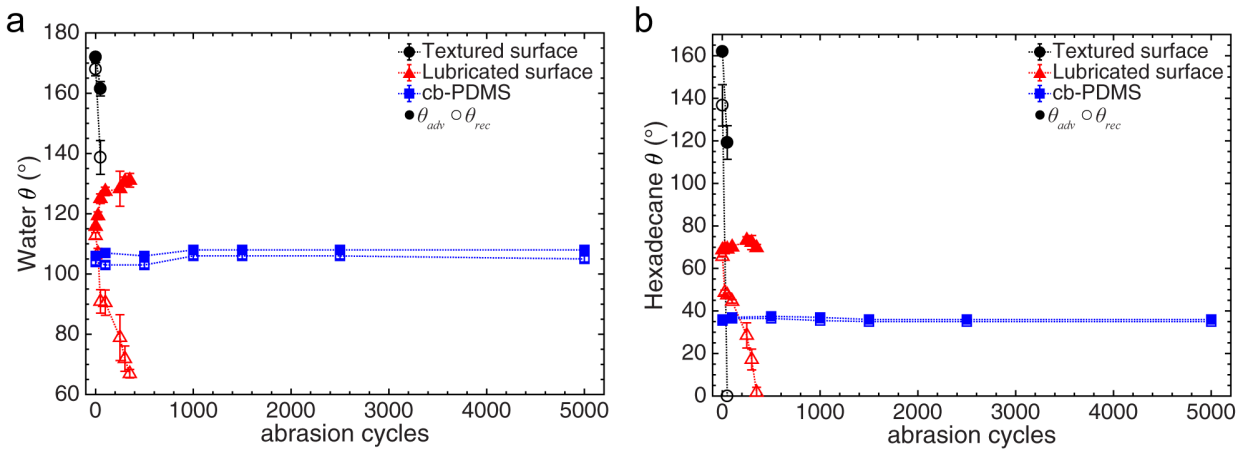

Figure 5.12: θ_a/θ_r of water and hexadecane on the capped bidentate PDMS surface (cb-PDMS) versus the number of linear Taber abrasion cycles. No significant degradation in θ or $\Delta\theta$ was observed.

5.5 Superfluorophobic Surfaces

A moving droplet with relatively high contact area on a smooth surface can exhibit an instability at its receding contact line. This instability can lead to 'pearling', pinching-off of the receding contact line leaving small satellite droplets on the surface. The minimum velocity for the onset of pearling is proportional to the droplet sliding velocity U, liquid viscosity η, liquid surface tension, and the receding contact angle, as $U \propto 2\gamma_{LV}(\theta_r)^3/\eta$. A high receding contact angle therefore strongly suppresses pearling.[237] Although the smooth b-PDMS and cb-PDMS films exhibited extremely low

$\Delta\theta$, θ_r with most low-γ_{LV} liquids remained relatively low. At high sliding velocities, droplets of these liquids were prone to leaving satellite droplets on the smooth PDMS films. This was especially true of the fluorinated liquids. However, cb-PDMS can be used to fabricate non-wetting textured surfaces to overcome this limitation. The only previous reported method for repelling fluorinated liquids demonstrated a metastable Cassie-Baxter state on microfabricated "doubly re-entrant" silicon features, even with liquids that completely wet silicon.[43] As the cb-PDMS has a non-zero contact angle with fluorinated liquids, cb-PDMS treated, flat-topped silicon micro-hoodoos, which are significantly simpler to fabricate, can also be used to repel fluorinated liquids in the Cassie-Baxter state (Figure 5.13).

Microfabrication of the micro-hoodoos was performed in the Lurie Nanofabrication Facility using standard protocols. A ~1μm thick layer of silicon dioxide was deposited with plasma-enhanced chemical vapor deposition (GSI Ultradep 2000 PECVD) on a silicon wafer. Standard photolithography procedure was used to define a square array of photoresist circles (Shipley SPR 220-3.0, 3μm thick) on the oxide layer, which was then selectively plasma-etched with C_4F_8 (STS APS DGRIE). The photoresist was stripped, leaving an array of SiO_2 circles on silicon. A standard Bosch process etch (STS Pegasus DRIE) was then used to anisotropically etch the exposed silicon, yielding pillars with vertical sidewalls and SiO_2 tops. The thin native oxide film on the pillar sidewalls was stripped with a brief dip in dilute buffered hydrofluoric acid. Isotropic etching was then used to undercut the SiO_2 caps (XeF_2 in Xactix Xetch X3), leaving a well-defined re-entrant micro-hoodoo structure (Figure 5.13). The final structures had 10μm diameter caps, were 30μm tall, and spaced at 45μm. This micro-hoodoo array was subsequently coated with b-PDMS using the procedure described above to render it non-wettable by water, oil, organic solvents, and fluorinated liquids. For example, droplets of perfluorodecalin displayed θ_a^*/θ_r^* = 165°/111°, and rolled from the surface without transitioning to the Wenzel state. Note that, on F-17-treated hoodoos, θ_a^*/θ_r^* = 163°/141° with water, and 166°/123° with hexadecane. However, both Krytox 103 and perfluorodecalin completely wetted the fluorosilanized texture, *i.e.*, θ_a^*/θ_r^* = 0°/0°.

5.6 Ongoing Work: Condensation Heat Transfer

Many critical industrial processes rely on the efficient condensation of steam, including power generation (85% of plants worldwide), and desalination (50%). Even relatively small improvements in heat-transfer efficiency during steam condensation would have a large impact on costs and energy savings. A large body of research has demonstrated that the heat-transfer coefficient (heat flux divided by the temperature gradient) during dropwise condensation can be an order of magnitude greater than that during condensation as a film.[207] This is because film-wise condensation creates a liquid barrier on the surface with low thermal conductivity, insulating the chilled surface from the hot vapor and drastically decreasing the driving force for further condensation. Continuous removal

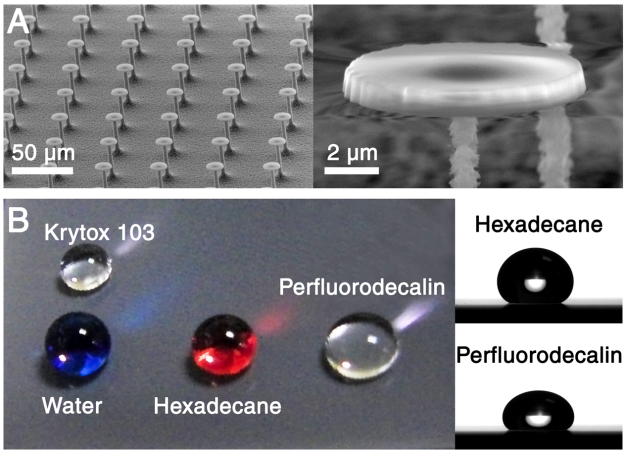

Figure 5.13: (*a*) SEMs of micro-hoodoo structures etched in silicon and treated with cb-PDMS. (*b*) A photograph of four different liquids on our cb-PDMS-treated micro-hoodoos. For water, θ_a^*/θ_r^* =163°/134°. For hexadecane, θ_a^*/θ_r^* = 168°/115°. For perfluorodecalin, θ_a^*/θ_r^* = 165°/111°. The insets are images from the contact angle goniometer measurement of hexadecane and perfluorodecalin droplets. The high viscosity of Krytox 103 prevented accurate dynamic contact angle measurements.

of the condensed liquid is critical for improving efficiency.

Water is dominant as a heat-transfer fluid, due to cost, but usage of hydrocarbon and silicone oils, cryogens, and fluorocarbons remains significant in heat exchange processes. The efficiency of numerous industrial processes could be improved by improving the heat transfer coefficient from condensation of these low-surface tension liquids in addition to water.[198] These surfaces could also be used to collect the liquid condensate from the vapor, for example to collect water from fog in areas where conventional water sources are restricted, or to recover solvents in industrial processes.[238] A low hysteresis omniphobic coating which is stable under hot vapor conditions is therefore strongly desirable. Studies demonstrating stable drop-wise condensation of non-aqueous, low-surface tension liquids remain quite limited, due to the challenge in maintaining low contact angle hysteresis and sufficiently high contact angles with these liquids to prevent film-wise wetting in saturated vapor conditions.

The thin, smooth, solid-state omniphobic spin-coated film reported in Section 4 appeared promising based on the preliminary testing with hexane and ethanol vapors under vacuum conditions in Section 4.3.3. However, its long term stability at elevated temperatures, especially in hot vapors of aggressive solvents, may be insufficient. The microcrystals of fluorodecyl POSS appear to melt and re-crystallize well below its degradation temperature as determined by TGA (> 350 °C, Figure 3.16). This effect significantly increases contact angle hysteresis by increasing roughness and chemical heterogeneity. Additionally, the presence of any insulating film thickness may significantly offsets any benefit gained from maintaining dropwise condensation. The grafted b-PDMS and cb-PDMS films, however, despite their lower initial contact angles, appear to retain them much better over time after exposure to heated solvents (Figure 5.11). We have fabricated an apparatus to quantitatively

measure the heat transfer coefficients of these surfaces when condensing water and other relevant solvents and to validate their long-term efficacy. Testing is ongoing on this grafted PDMS surface and others.

5.7 Ongoing Work: Substrate-Independent, Durable, Omniphobic Coatings

The key drawback of the surface treatment described here is the restriction to hydroxide-rich substrates compatible with silanes. In condensation heat exchangers, for instance, the predominant material used is copper, whose oxide is far less reactive to silanes. It is highly desirable to combine the substrate-independent application methods usable with the smooth omniphobic coating in Chapter 4 with the temperature and solvent resistance of the grafted PDMS chains in a coating with improved durability.

We hypothesized that producing a densely cross-linked PDMS network which resists swelling, even by solvents that favorably interact with PDMS, will yield similar surface characteristics to grafted PDMS chains on a hard substrate. Compared to conventional PDMS elastomers, such as Dow Corning Sylgard 184 which is commonly used in microfluidics research, some harder formulations can repel low-surface tension liquids such as hexadecane and ethanol with contact angle values similar to those reported for the grafted PDMS in Table 5.1. One such formulation, referred to as hPDMS, was previously reported in the literature for use as a nanoimprint lithography stamp.[239,240] This formulation relies on platinum-catalyzed hydrosilylation (Figure 5.14a) to create a densely cross-linked network from a vinylmethylsiloxane-dimethylsiloxane copolymer (Gelest VDT-731) and a methylhydrosilane-dimethylsiloxane (Gelest HMS-301) (Figure 5.14b). A coating produced from a 61.5:38.5 wt.% mixture of these components, with a platinum catalyst, does indeed show low contact angle hysteresis with water, hexadecane, and ethanol (water θ_a/θ_r = 108°/104°, hexadecane θ_a/θ_r = 34°/32°, ethanol θ_a/θ_r = 36°/31°). However, the key drawback of such as system is its low tensile strength (0.5–0.75 MPa) and moderate elongation to breakage (30–40%).[241] In fact, drop-cast coatings thicker than approximately 25 μm were found to spontaneously crack due to shrinkage stresses after curing, and could easily be scratched with a fingernail. Conventional coating materials such as epoxies and polyurethanes possess far higher toughness.

Ongoing efforts are focused on improving the liquid-repellence and durability of this system to exceed that of the smooth omniphobic coating reported in Chapter 4. Replacing the methylhydrosilane-dimethylsiloxane linear copolymer with a hydride-functional quaternary siloxane resin ("Q resin", Figure 5.14c), a reinforcing agent, resulted in some improvement in contact angle hysteresis (water θ_a/θ_r = 108°/104°, hexadecane θ_a/θ_r = 34°/33°, ethanol θ_a/θ_r = 36°/32°) and strength (the films were significantly less prone to propagating cracks due to thermal stress or indentation). However, the abrasion resistance remained low, and this is a key challenge as even light surface scratching

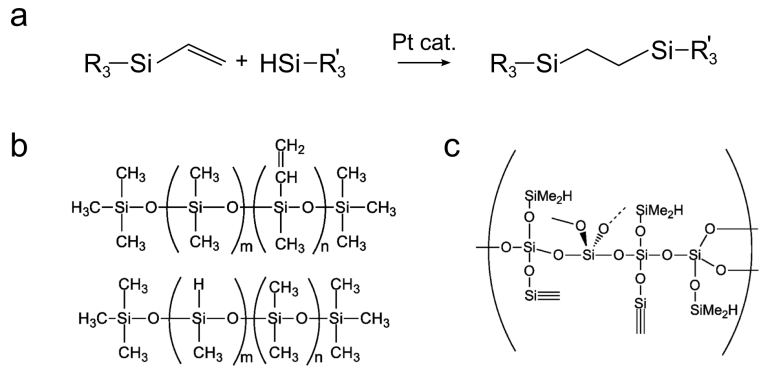

Figure 5.14: Structures of components that may yield a durable, substrate-independent omniphobic coating based on highly cross-linked PDMS. (*a*) Schematic of the platinum-catalyzed hydrosilylation reaction. (*b*) Vinyl and hydride dimethylsiloxane co-polymers. (*c*) Hydride-functionalized quaternary siloxane resin, a reinforcing agent.

significantly increases the roughness and causes complete wetting of low-γ_{LV} liquids. The relatively high surface energy of PDMS compared to the highly fluorinated smooth film in Chapter 4, (~20 mN/m versus ~9 mN/m) means that maintaining low surface roughness is more important for maintaining liquid repellence after abrasion.

Conventionally, the mechanical properties of siloxanes are improved by incorporating silica particles. For this application, the effective dispersion of nanoparticles is especially critical to maintaining high transparency, low surface roughness, and low $\Delta\theta$. Silica fillers are generally modified with hydrophobic silanes to assist dispersion, such as hexamethyldisilazane (HMDS), or reactive functional groups that bond them to the matrix. Rather than inorganic nanoparticles, polyhedral oligomeric silsesquioxane (POSS) molecules, similar to those used in Chapters 3 & 4, could be incorporated as essentially molecular-scale silica reinforcement.[242] As with the silica particles, they may incorporate unreactive hydrophobic moieties or reactive functional groups. Some nanocomposites prepared with POSS and various polymer matrices have demonstrated improved thermal and mechanical properties.[242–247] Finally, the PDMS matrix could be copolymerized with other, tougher, non-siloxane monomers, such as epoxies or urethanes. The key challenge with all of these approaches is the uniform dispersion of the fillers such that the coating mechanical properties are enhanced, while the $\Delta\theta$ remains unaffected. This is especially challenging to accomplish with PDMS, and will be the focus of future work.

5.8 Conclusions

Surfaces with flexible grafted molecules exhibiting near-zero contact angle hysteresis show promise in a wide range of fields where minimal adhesion to liquids and solids is desirable. We developed a rapid, single-step technique to graft flexible PDMS chains to silanol-containing surfaces via exposure to a vapor of a volatile, bi-functional, chlorine-terminated siloxane precursor at room temperature. The resulting films are stable even in relatively harsh environmental conditions. These

tethered PDMS films are the first smooth surfaces to repel fluorinated solvents with low contact angle hysteresis, in addition to a broad range of other liquids with varying surface tension and polarity. Due to their flexible, amorphous nature enabling interfacial slippage, these surfaces also dramatically reduce adhesion to various types of solids as compared to a perfluorinated monolayer. This coating, therefore, is useful to prevent fouling by both liquids and solids on a broad range of surfaces used in architecture, transportation, biomedical, microfluidic, and photolithography applications. Future work is focused on using these surface-treatments to demonstrate efficient dropwise condensation heat transfer with low surface tension liquids, as well as attempting to replicate their properties in a substrate-independent, durable, scalable coating.

5.9 Acknowledgements

We thank Dr. Ki-Han Kim and the Office of Naval Research (ONR) for financial support under grant N00014-12-1-0874. We also thank Dr. Charles Y. Lee and the Air Force Office of Scientific Research (AFOSR) for financial support under grants FA9550-15-1-0329 and LRIR-12RZ03COR. We also thank the National Science Foundation and the Nanomanufacturing program for supporting this work through grant #1351412. K. Golovin thanks the Department of Defense (DoD) for a National Defense Science & Engineering Graduate (NDSEG) Fellowship.